

# Microglia and astrocytoma cells express alkylindole-sensitive receptors

---

Susan Fung

A dissertation submitted in partial fulfillment of the requirements for the degree of  
Doctor of Philosophy

University of Washington

2014

Reading Committee:

Dr. Nephi Stella, Chair

Dr. Gwenn Garden

Dr. Neil Nathanson

Program Authorized to Offer Degree:

Neurobiology & Behavior

© Copyright 2014

Susan Fung

University of Washington

### **Abstract**

Microglia and astrocytoma cells express alkylindole-sensitive receptors

Susan Fung

Chair of the Supervisory Committee:

Professor Nephi Stella

Department of Pharmacology

Two cannabinoid (CB) receptors, CB<sub>1</sub> and CB<sub>2</sub>, have been identified at the molecular level. Evidence suggests that other cannabinoid and cannabinoid-like receptors remain to be identified. Using newly developed compounds, our lab has identified receptors sensitive to alkylindoles (AI) which exhibit a distinct pharmacological profile from CB<sub>1</sub> and CB<sub>2</sub> receptors and are expressed by both microglia and astrocytomas.

Radioligand binding data show that WIN-2, and novel analogues, ST-11 and ST-48, compete for [<sup>3</sup>H]WIN-2 binding in DBT mouse astrocytoma cells and primary microglia in culture, while classic cannabinoid ligands did not. In microglia, ST-11 and ST-48 increase intracellular cAMP levels, suggesting that AI receptors are GPCRs that couple to G<sub>s</sub>.

As resident immune cells of the CNS, microglia play many roles in maintaining homeostasis in a healthy brain. AI analogues inhibit both basal and ATP-stimulated microglia cell migration. The compounds did not affect cell viability, yet they did inhibit cell proliferation stimulated by macrophage colony stimulating factor (M-CSF). Interestingly, AI analogues did not modulate effector proteins that characterize M1 or M2 phenotypes.

AI analogues also inhibited DBT cell migration, though with lower efficacy. In contrast to microglia, AI analogues did reduce cell viability and basal cell proliferation, suggesting that AI-sensitive receptors expressed by cancer cells may be an effective target to reduce tumor growth. In vivo study of ST-11 formulated in liposomes show that tumor

volume was reduced while microglia reactivity was increased. Further study of Al analogues is needed to increase understanding of this phenomenon.

## Table of Contents

Abstract.....	3
Dedication.....	7
INTRODUCTION: Targeting endocannabinoid signaling in tumor-associated macrophages as treatment for glioblastoma multiforme.....	8
Abstract.....	8
GBM: origin, allies, and fate .....	9
Current treatment options for GBM patients .....	9
Classification, origin, and genetic profile of GBM tumors .....	9
Blood brain barrier (BBB) integrity and brain tumor microenvironment .....	11
Multiple activation states and phenotypes of microglia .....	13
Endocannabinoid and cannabinoid-like signaling in TAMs and GBM .....	14
Cannabinoid receptors .....	14
Cannabinoid ligands .....	15
eCB signaling in microglia.....	17
Novel targets for GBM therapeutics - the next line of treatment.....	19
CHAPTER 1: Alkylindole-sensitive receptors modulate microglial cell migration and proliferation .....	21
Abstract.....	21
Introduction.....	21
Results .....	23
Microglia express functional AI-sensitive receptors.....	23
AI-sensitive receptors control microglial cell migration and proliferation.....	25
AI receptors do not control microglial cell M1 and M2 phenotypes .....	29
Discussion .....	32
Acknowledgments .....	34
Materials and Methods .....	34
CHAPTER 2: In vivo evidence that alkylindole compounds promote apoptosis in astrocytomas independently of CB <sub>1</sub> and CB <sub>2</sub> receptors.....	37
Abstract.....	37
Introduction.....	37

Results .....	38
The mouse astrocytoma cell line, DBT, expresses AI-sensitive receptors and lack CB <sub>1</sub> and CB <sub>2</sub> receptors.....	39
AI receptors control cell migration, proliferation, and viability .....	42
Solubility, pharmacokinetic profile, and safety of ST-11 .....	45
ST-11 induces apoptosis in the DBT syngeneic mouse model of astrocytoma .....	49
Tumor-associated macrophages respond to ST-11 treatment .....	51
Discussion .....	53
Materials and Methods .....	54
Chapter 3: Conclusions .....	57
Summary .....	57
Future directions.....	57
Closing remarks.....	59
References .....	61

## Dedication

This is dedicated to Alfred. Thank you for not letting me go hungry on late nights, organizing game night when a moment of levity was needed, for encouraging me to run when I needed a mental reset. Thanks for the hugs of victory and of solace, for letting me cry. Thank you for cheering me on.

## INTRODUCTION: Targeting endocannabinoid signaling in tumor-associated macrophages as treatment for glioblastoma multiforme

Adapted from Fung, S, Stella N. 2014 Targeting endocannabinoid signaling in tumor-associated macrophages as treatment for glioblastoma multiforme. *WIREs Membr Transp Signal* 3:39-51

### Abstract

Glioblastoma multiforme (GBM) is the most common form of primary brain tumor and is diagnosed in approximately 10,000 people each year in the United States alone. No cure for this type of cancer exists, and the current standard of care treatments provide little benefit and are associated with debilitating side effects. Recent evidence shows that a large number of tumor-associated macrophages (TAMs) invade the GBM tumor mass and secrete factors that directly and indirectly promote tumor growth. TAMs express a panel of unique receptors that could be targeted for therapeutic benefit. One such receptor, cannabinoid receptor 2 (CB2), is a member of the endocannabinoid (eCB) signaling system, and its activation has been shown to tightly control the migration and phenotype of both macrophages and microglia. Additional receptors, also engaged by eCBs and cannabinoid-like compounds, are expressed by macrophages and microglia. These receptors also control cell migration and phenotype, but exhibit distinct pharmacological profiles and operate through a different mechanism of action. Strong evidence accumulated over the past decade indicates that membrane receptors expressed by TAMs represent novel targeting opportunities to treat GBM tumor progression. Here we review studies that significantly increased our understanding of the molecular mechanism of action of receptors engaged by eCBs and cannabinoid-like compounds expressed by GBM tumor cells and TAMs. This evidence provides a strong rationale for developing new therapeutics that target the eCB signaling of TAMs for the treatment of GBM while minimizing the typical side effects associated with standard care.

## GBM: origin, allies, and fate

### Current treatment options for GBM patients

GBM tumors are the most severe, aggressive and common form of primary brain tumor, accounting for one percent of cancer diagnoses in the U.S. each year<sup>1</sup>. Epidemiological data gathered between 2005 and 2009 show that the incidence of GBM is 6.5 per 100,000 individuals, and that this type of cancer afflicts slightly more men (7.7 per 100,000) than women (5.4 per 100,000)<sup>2</sup>. It is estimated that roughly 20,000 new cases of GBM will be diagnosed in 2013 with an average age at diagnosis of 64<sup>1,2</sup>. With the population living progressively longer lives, this fatal disease should be increasingly diagnosed in the coming decades.

The first step in the current standard of care treatment for this disease consists of surgical resection to debulk as much of the tumor mass as possible. Additionally, with the skull kept intact, tumor removal can be augmented by gamma-knife surgery (GKS). There are several daunting limitations to the initial resection of the tumor mass. First, not all GBM tumors can be safely treated by GKS because of their size (maximum size for GKS treatment being 35-40 mm) and the intervention depends on whether or not the tumor location is close to vital brain structures<sup>3</sup>. Second, in the best case scenario, although surgeries remove 95-97% of the GBM, the remaining percentage of GBM cells typically leads to tumor recurrence. In fact, a multi-center clinical trial that evaluated the use of GKS before traditional external beam radiotherapy plus carmustine (BCNU) chemotherapy showed that GKS did not improve overall survival<sup>4</sup>.

Radiotherapy and chemotherapy are the next steps in the standard of care treatments following debulking and are typically prescribed for patients younger than 70 years of age<sup>5,6</sup>. For elderly patients, either radiation or chemotherapy-only treatment is recommended. Commonly prescribed chemotherapeutics for GBM are the DNA alkylating agents BCNU and temozolamide (TMZ)<sup>7</sup>. However, certain GBM types do not respond to TMZ as they express the MGMT gene, leading to increased production of the enzyme that reverses the alkylating effects of TMZ, and resulting in chemotherapeutic resistance. Furthermore, both radiotherapy and chemotherapy are associated with severe side-effects principally because these chemotherapeutics indiscriminately damage tumor and healthy cells. As a result, patients undergoing such treatment require additional medications to alleviate these side-effects. Considering the serious limitations associated with these standard of care options for GBM patients, there is an urgent need for novel and less toxic therapeutic approaches that will rapidly and efficiently treat this type of deadly cancer.

### Classification, origin, and genetic profile of GBM tumors

GBM is classified as a World Health Organization (WHO) grade IV astrocytoma. Under the WHO grading system, astrocytomas are categorized in four grades based on histopathological features, including hypercellularity, pleomorphism, and pseudopalisading necrosis, this last feature being typical of GBMs<sup>1,8</sup>. More recently, a new classification system has been introduced by The Cancer Genome Atlas Network based on gene expression data and factor analysis. It is hypothesized that different types of GBM tumors arise from different causes or from different GSC cells of origin. Accordingly, GBM tumors have been subcategorized into four types: classical, mesenchymal, neural, and proneural<sup>9</sup>. The classical type is characterized by an amplification of chromosome 7 (where the oncogene epidermal growth factor receptor [EGFR] and proto-oncogene mesenchymal-epithelial transition factor receptor [MET] are located) and a loss of chromosome 10 (where the tumor suppressor phosphatase and tensin homolog [PTEN] is located). EGFR amplification is a common occurrence in a majority of these samples, whereas tumor protein 53 (TP53) mutations are rarely present, an interesting finding considering that TP53 is thought to be the most common mutation found in GBM<sup>10</sup>. The mesenchymal type shows low expression of neurofibromin 1 (NF1) in comparison to other subtypes and prominent expression of the mesenchymal markers chitinase-3-like protein 1 (CHI3L1) and MET. This study also reported high expression of members of the tumor necrosis factor (TNF) and NF- $\kappa$ B pathways, TNF receptor type 1-associated DEATH domain (TRADD), RELB, and TNF receptor superfamily member 1A (TNFRSF1A), which corresponds to the higher amount of necrosis and inflammatory molecules found in these GBMs. The neural type is defined by typical neuronal marker expression, such as neurofilament light polypeptide (NEFL), gamma-aminobutyric acid receptor subunit alpha-1 (GABRA1), and synaptotagmin-1 (SYT1). Lastly, the proneural type is typified by two mutations: platelet-derived growth factor receptor alpha (PDGFRA) and isocitrate dehydrogenase 1 (IDH1). Furthermore, several genes associated with oligodendrocytic cell development are also highly expressed by this type of GBM. Interestingly, it is the proneural subtype that associates with the highest rate of TP53 mutations. The information gained by these studies provides a remarkable step towards providing personalized and effective treatments to GBM patients, with the hope of tailoring therapies that will provide better treatment.

GBMs are heterogenous in nature and are likely to originate from GBM stem cells (GSCs). GSCs express CD133, can differentiate into various cell types when studied *in vitro*<sup>11</sup>, and suffice for initiating tumorigenesis<sup>11-14</sup>. Specifically, when implanted into the mouse brain, CD133+ GSC spheres generated tumors while non-sphere-forming cells did not, providing evidence of the self-renewal properties of GSC spheres and of the mechanism of tumor recurrence. Supporting this notion of self-renewal, levels of CD133 mRNA were higher in recurrent GBM samples compared with primary tumors<sup>13</sup>. CD133+ GSCs are more resistant to conventional chemotherapeutics than CD133-

GSC cells<sup>13</sup> and any novel therapeutic approaches must accordingly target both CD133+ and CD133- cells to successfully treat these tumors<sup>12,15</sup>. Indeed, although CD133- GSC cells are not as proliferative as CD133+ GSCs, they still are tumorigenic after implantation in mice and thus should also be targeted by therapeutics<sup>12</sup>. In summary, multiple lines of evidence exist that suggest that GSCs are likely the source of GBM tumors and are a culprit of drug resistance.

### Blood brain barrier (BBB) integrity and brain tumor microenvironment

One difficulty of delivering therapeutics to the CNS is passing the blood brain barrier (BBB)<sup>16,17</sup>. The brain is considered an immune-privileged site as the BBB restricts access to peripheral molecules and cells, circulating immune cells in particular. Specifically, the BBB is comprised of endothelial cells connected through tight junctions that create a semi-impermeable barrier limiting the entry of circulating immune cells and mediators into the brain and spinal cord parenchyma<sup>16,17</sup>. Furthermore, cells forming the BBB are equipped with active efflux transporters that control the entry of various drugs<sup>18,19</sup>. With this isolated setting, the CNS depends mainly on microglia as the first line of defense to detect and respond to pathogens and cancer. However, under pathological conditions the BBB may be compromised, allowing for the influx of monocytes, other leukocytes, and a plethora of potentially harmful molecules that might further damage the brain parenchyma<sup>20,21</sup>.

GBM progression leads to varying degrees of BBB breakdown<sup>22</sup> and may be due to the high levels of vascular endothelial growth factor (VEGF) secreted by GBM cells which is known to disrupt BBB permeability<sup>20</sup>. Specifically, based on immunohistochemical analysis of human astrocytoma samples, serum proteins are detected in the brain parenchyma surrounding the tumor (also known as “the tumor rim”)<sup>23</sup>. In comparison, the same study showed that such serum proteins are exclusively localized to the meninges and within blood vessels of healthy brain tissue. The tumor rim is often also associated with edema, suggesting that glial cell dysfunction may reach a larger area than the tumor mass per se<sup>24</sup>. For example, both aquaporin-4 up-regulation and swollen cell bodies of GFAP+ glial cells are detected in the tumor rim<sup>24</sup>. Thus, the BBB disruption is associated with an increase in the influx of immune cells that interact with a large number of tumor-associated macrophages (TAMs)<sup>25-28</sup>. Landmark studies show that the number of the immune cells in and around the tumor correlate with severity of the disease, indicating that TAMs represent a cell population that should strategically targeted for GBM therapy<sup>27</sup>.

### Microglia: the sentinels of the CNS

Microglia are often referred to as “the resident macrophages of the brain” and are known to play roles in both innate and adaptive immune responses in the brain. Microglia detect pathogens and cell injuries, combat pathogens by releasing free radicals, phagocytose cell debris, present antigens to invading immune cells, and release mediators that modulate neighboring cells and invading immune cells<sup>29,30</sup>. In healthy brain, they exhibit a ramified morphology and constantly use their processes to survey the local brain parenchyma<sup>31,32</sup>. Until recently, it was thought that microglial cells derive from hematopoietic stem cells; however, recent evidence shows that they originate from primitive myeloid cells in the yolk sac between E7.25 and E7.5 in mice<sup>33</sup>. This short time window during embryogenesis precedes the time window of hematopoiesis and clearly separates microglia from the bone marrow-derived monocytes that eventually mature to tissue macrophages<sup>33</sup>. These new findings open a set of novel hypotheses, including one that proposes a fundamental difference in how resident microglia and invading macrophages interact with GBM cells and affect tumor growth.

### Factors used by GBMs to recruit microglia and TAMs

Tumor cells secrete both chemoattractants and growth factors that promote the recruitment of microglia and circulating monocytes, and thus determine the number and phenotype of microglia and TAMs invading the tumor mass. Select chemokines have been involved in this process, including monocyte chemoattractant protein-1 (MCP-1)<sup>34,35</sup> and/or MCP-3<sup>36</sup>, VEGF<sup>37,38</sup>, and hepatocyte growth factor/scatter factor (HGF/SF)<sup>39,40</sup>. Tumor cells also secrete growth factors, such as granulocyte colony-stimulating factor (G-CSF) and granulocyte-macrophage-CSF (GM-CSF), both of which are known to induce microglial cell proliferation<sup>41</sup>.

Microglia and TAMs secrete a wide array of immune mediators. For example, they release interleukin-10 (IL-10) that contributes to establishing an immunosuppressive environment<sup>42,43</sup>, as well as matrix metalloproteases that break down extracellular matrix and aid tumor propagation<sup>44</sup>. Both microglia and TAMs also secrete VEGF, which promotes angiogenesis and ensures ample access to the nutrients and oxygen needed to maintain and promote cancer cell survival<sup>45</sup>. VEGF also acts as a chemoattractant for VEGFR-1-expressing microglia and macrophages<sup>37,38</sup> and contributes to tumor growth, yet it has become increasingly clear that targeting a single factor is impractical and provides little benefit. With this evidence in hand, the field of brain cancer research is now dedicating significant effort to better understanding the role of microglia and macrophages invading the GBM tumor mass, as well as is testing whether drugs known to limit the migration of TAMs provide therapeutic benefit for patients diagnosed with these tumors.

## Multiple activation states and phenotypes of microglia

Microglia phenotype is highly malleable and adjusts depending on the stimuli and disease state encountered in the brain parenchyma<sup>46</sup>. When homeostasis is disrupted, microglial cells may adopt at least three broadly-classified phenotypes: an M1 phenotype (or classical activation), an M2 phenotype (or alternative activation), or a tumor-associated phenotype, which encompasses facets of both M1 and M2<sup>46,47</sup>. This evidence challenges the previous dogma stating that microglia undergo simple bimodal phenotypic changes from resting to activated. Note that the mechanism by which microglia return to a patrolling phenotype upon resolution of a neurotoxic event – if at all – is poorly understood. Several studies indicate that IL-4 and transforming growth factor- $\beta$  (TGF- $\beta$ ) may play a role in their resolution<sup>48</sup>, but a growing consensus suggests that microglia may retain some amount of memory of their previous activation state, which may confer an advantage in the future if a similar event occurs<sup>48,49</sup>. This same result however, may be detrimental as the cells may contribute to the recurrence of undesired events, such as tumors.

With regard to GBM tumors, TAMs assume phenotypes typified by specific markers. A series of key studies showed that the TAM phenotype lies between the M1 and M2 phenotypes, suggesting a tailored response to GBM tumors. When analyzing the phenotype of TAMs in an orthotopic rat GBM model, Badie and Schartner found that CD45+/CD11b+ cells (classified as invading macrophages) were primarily located within the tumor mass, whereas microglia (CD45-/CD11b+ cells) were located throughout the tumor and brain parenchyma<sup>25</sup>, a distribution that mirrors what is found in human GBM samples<sup>50</sup>. Note that these claims are based on the assumption that the expression of the CD45/CD11b markers remains stable over time<sup>51</sup>. GBM cells also secrete TGF- $\beta$ <sup>52,53</sup>, which promotes an immunosuppressive phenotype in TAMs by down-regulating major histocompatibility complex II (MHC II) and other antigen presenting molecules<sup>54</sup>. Remarkably, in TAMs isolated from patients with GBM, both MHC II and toll-like receptors (TLRs) are expressed; yet the co-stimulatory surface markers (such as CD80, CD86, CD40) are not. In fact, these cells do not produce pro-inflammatory cytokine production except for IL-12<sup>28</sup>. In line with these findings, TAMs are poor antigen presenting cells when studied in vitro<sup>55</sup>. Additional markers change their expression in TAMs, and understanding their specific role in cell function would help enhance our understanding of the phenotype adopted by TAMs. For example, Iba-1, which plays a role in calcium homeostasis<sup>56</sup> and phagocytosis, is commonly used as a marker to identify cells belonging to the monocytic lineage. Other surface markers commonly used

to identify this cell population are CD11b and CD18, which are subunits of the integrin Mac-1, as well as F4/80, all proteins that control and facilitate cell adhesion<sup>56,57</sup>. CD68 is another commonly used protein marker to indicate phagocytosis<sup>56</sup>. When attempting to characterize the phenotype of cells belonging to the monocytic lineage, a combination of markers that detect MHC II, iNOS and other M1 markers indicate a pro-inflammatory (classical) phenotype, and markers that detect CD204 and CD206 and other M2 markers indicate an anti-inflammatory (alternative) phenotype. Thus co-immunostaining with a panel of cell surface markers should offer an opportunity to study the dynamic change in the phenotype adopted by TAMs, and how such changes in TAM phenotype are affected by regimented therapeutic treatment.

In summary, GBM is a devastating cancer that remains uniformly fatal. The recent discovery that GBM can be further classified into four GBM types based on gene expression profiles should help guide the next generation of therapeutics that will directly target the cancer cells and stem cells. A promising new treatment venue is to target TAMs as these cells invade the GBM tumor mass and have been shown to significantly promote tumor growth. In the next section, we will first introduce our current understanding of the eCB signaling system and then propose a rationale for targeting eCB signaling in TAMs as a novel therapeutic approach to treat GBM.

## Endocannabinoid and cannabinoid-like signaling in TAMs and GBM

### Cannabinoid receptors

Two cannabinoid (CB) receptors have been identified at the molecular level<sup>58,59</sup>, and both receptors, CB<sub>1</sub> and CB<sub>2</sub>, are G protein-coupled receptors (GPCRs). CB<sub>1</sub> is one of the most widely expressed GPCRs in the brain and has particularly high expression levels in GABAergic neurons<sup>60</sup>. However, it is CB<sub>1</sub> on glutamatergic neurons that underlie most of the cannabinoid-induced behaviors, as well as couple to G proteins more effectively than CB<sub>1</sub> on GABAergic neurons<sup>61</sup>. Both CB<sub>1</sub> and CB<sub>2</sub> receptors couple to G<sub>i</sub> proteins and regulate ion channels and second messengers, such as cAMP and ERK kinase. Thus, CB<sub>1</sub> mediates the psychotropic effects of  $\Delta^9$ -tetrahydrocannabinol (THC), the principal psychoactive component of the Cannabis plant. CB<sub>2</sub> receptors share 44% homology with CB<sub>1</sub> and couple to G<sub>i</sub> but likely not G<sub>o</sub> proteins<sup>59,62</sup>. The expression level of CB<sub>2</sub> receptors is low in the brains of healthy individuals<sup>63-65</sup> but is considerably up-regulated in microglia under chronic pro-inflammatory and autoimmune conditions<sup>63,66,67</sup>. CB<sub>2</sub> receptors control several immune functions carried by microglia, for example, by tightly regulating actin polymerization, migration, cell phenotype and pro-inflammatory cytokine release from these cells<sup>63,66,68,69</sup>. Thus, cannabinoid

receptors are likely to play an integral part in regulating fundamental functions of microglia, macrophages, and TAMs.

## Cannabinoid ligands

Cells produce eCBs on-demand that activate CB receptors and regulate specific cell functions. Arachidonylethanolamine (anandamide, AEA) acts as a partial agonist at CB receptors, but 2-arachidonoyl glycerol (2-AG) acts as a full agonist<sup>70,71</sup>. A large panel of synthetic molecules that either activate or antagonize CB receptors have been developed over the past 30 years and can be categorized into five main classes<sup>72,73</sup>. Classical cannabinoids are tricyclic-dibenzopyran derivatives, including THC and HU-210. Although both compounds are structurally similar and belong to the same class, THC has much lower affinity to CB<sub>1/2</sub> than HU-210 and acts as a partial agonist. Members of the non-classical group of compounds structurally resemble those of the classical group but lack the pyran ring. A prototypical member of this family is CP-55940 (CP), which is a potent full agonist at both CB receptors. The third group of molecules is the aminoalkylindoles, of which WIN 55,212-2 (WIN-2) is a member. This compound also acts as a potent full agonist at CB<sub>1</sub> and CB<sub>2</sub> receptors despite being structurally very different from the classical and non-classical compounds. The fourth group of compounds is the eicosanoids or derivatives of arachidonic acid which include the eCBs 2-AG and AEA. Finally, the last class is made up of diarylpyrazoles including SR141716 (SR1) and SR144528 (SR2)<sup>74,75</sup>, which act as inverse-agonists at CB<sub>1</sub> and CB<sub>2</sub> receptors, respectively.

## eCB signaling in astrocytomas and the use of CB ligands in treating GBM

The practice of utilizing cannabis as medicine is not new; in fact, the plant has been used medicinally for thousands of years<sup>76</sup>. Today, patients continue to use cannabis and specifically formulated cannabinoid compounds to stimulate appetite, alleviate pain, nausea, and vomiting associated with cancer, chemotherapy treatment, and in some cases neurodegenerative diseases<sup>77,78</sup>. The study of cannabinoids as antitumor agents began in 1975, when Munson et al. showed that growth of Lewis lung adenocarcinomas was delayed by oral administration of cannabinoids<sup>79</sup>. Many landmark studies ensued, including a remarkable set of studies on the effect of CB drugs on GBM pathogenesis. For example, THC and WIN-2 improved lifespan in most rats implanted with C6 cells, a rat glioma cell line; in some cases, the tumor was completely eradicated<sup>80</sup>. There is evidence for the expression of CB<sub>1</sub>/CB<sub>2</sub> receptors in tumor cells as measured by Western blot<sup>81</sup>, although the specificity of the CB<sub>2</sub> antibodies used in these studies

remains to be validated. Accordingly, the mechanisms by which cannabinoid drugs eliminate tumors are only beginning to be understood and require further research.

In vitro studies suggest that the cytotoxic effect that cannabinoids exert on GBM cells may require ERK activation<sup>80,82,83</sup>. We have shown that apoptosis induced by CB drugs depends on the expression level of CB receptors in astrocytoma cells<sup>83</sup>. Interestingly, low concentrations of CP induce apoptosis in cells expressing low levels of CB<sub>1</sub> receptors in an ERK-dependent manner. Cells that express high levels of CB<sub>1</sub> or CB<sub>2</sub> receptors do not promote apoptosis in response to CB agonists because these receptors now couple to pro-survival AKT signaling mechanisms. Here, it is important to emphasize that high concentrations of CP also induced apoptosis in cells lacking CB receptor expression, indicating that these compounds are capable of activating the ERK pathway independently of CB<sub>1</sub> and CB<sub>2</sub> receptors. These results also indicate that these receptors are sensitive to CB drugs, but remain uncharacterized with respect to their molecular identity, coupling mechanism, and pharmacological profile. Another study found that CBs, notably THC, induces autophagy in glioma cells by up-regulating the stress factor p8<sup>84</sup>. This leads to tribbles-homologue 3 (TRIB3) inhibiting AKT inhibiting mammalian target of rapamycin complex 1 (mTORC1) which can then initiate autophagy and autophagy-mediated cell death<sup>78,84</sup>. A study was also conducted addressing the effect of cannabinoids specifically in GSCs and found that multiple components of the eCB signaling system, including CB<sub>1</sub> and CB<sub>2</sub> receptors, were present<sup>85</sup>. Treating these cells with a selective CB<sub>1</sub> or CB<sub>2</sub> agonist increased markers of glial and neuronal differentiation in vitro and significantly decreased flank tumor volume when compared to controls<sup>85</sup>. Despite these promising results from in vitro and murine models, a clinical study using THC on patients with recurrent GBM did not show a significant improvement in survival over the standard regimen of TMZ<sup>81</sup>. It should be noted however, that this was a safety study that remained underpowered to ascertain treatment efficacy. In considering future clinical studies, the pathogenesis of recurrent GBM is likely to be different from primary or secondary GBM and variations in drug sensitivity may be related to changes in the expression levels of various genes, including transporters that allow for the development of drug resistance<sup>86</sup>. In response to this concern, one may propose combinations of cannabinoid compounds and the formulation of optimal treatment regimens to foster synergistic effects between various cannabinoids<sup>82</sup>. An added advantage to combining cannabinoids such as THC with cannabidiol (CBD) is the benefit of obtaining enhanced anticancer therapy and concomitantly reducing psychotropic effects<sup>87</sup>.

Other promising eCB targets are the CB<sub>2</sub> receptors expressed by endothelial cells of the BBB located in an area undergoing an inflammatory response. In this area, circulating immune cells adhere to endothelial cells, and this response is commonly interpreted as

BBB disruption. Recent evidence shows that CB<sub>2</sub> receptor agonists both reduce immune cell adherence to endothelial cells and increase the tight junction protein levels, together suggesting that these drugs should promote the BBB to regain integrity and consequently reduce leakiness<sup>88,89</sup>. Whether a similar response is induced by CB<sub>2</sub> agonist on the BBB in GBMs remains to be tested but is likely since this microenvironment is largely immunosuppressive. In fact, cannabinoid drugs should further help contain tumor growth by limiting the number of immune cells that invade the GBM tumor mass. One disadvantage of such response would be that it also limits the invasion of activated immune cells capable of combating the GBM and GCS cells.

### eCB signaling in microglia

Under healthy conditions in the CNS, microglia are thought to express low levels – if any – of CB<sub>2</sub> receptors. However, when homeostasis in the CNS is disrupted by specific types of injuries, microglia may up-regulate CB<sub>2</sub> receptor expression<sup>63</sup>, and activation of these receptors by selective compounds promote an anti-inflammatory phenotype<sup>90</sup> while suppressing a pro-inflammatory activation<sup>69</sup>. Results from in vitro studies indicate that when microglia up-regulate CB<sub>2</sub> receptors, production of both eCBs AEA and 2-AG is increased, enabling modulation of cell migration<sup>68,91–93</sup>. Microglia treated with AEA reduced the production of pro-inflammatory cytokines IL-12 and IL-23<sup>67</sup>. This anti-inflammatory response triggered by an eCB involves MKP-1, -3 which lowers p-ERK expression and TNF- $\alpha$  production<sup>90</sup>, as well as the JAK/STAT signaling pathway<sup>69</sup>. Romero-Sandoval et al. found that CB<sub>2</sub> activation, most likely through the inhibition of p-ERK, negatively regulated cell migration<sup>90</sup>. One may hypothesize that cannabinoid treatment will also result in an anti-inflammatory phenotype in TAMs of GBMs, but such hypothesis remains to be directly tested.

### Cannabinoid-like receptors expressed by both microglia and astrocytomas

It is now clear that CB compounds activate a number of receptors that remain uncharacterized with respect to their molecular identity, coupling mechanism and pharmacological profile. For example, WIN-2 and AEA stimulate [<sup>35</sup>S]-GTP $\gamma$ S binding and modulate synaptic transmission in CB<sub>1</sub> knockout mouse brain<sup>94–97</sup>. An additional set of evidence for the existence of such receptors comes from experiments performed on microglial cells in vitro. Here, lipids closely related to eCBs dose-dependently regulate microglia migration, and yet, it is known that they do not bind to CB<sub>1</sub> or CB<sub>2</sub> receptors<sup>91</sup>. For example, palmitoylethanolamide (PEA) is structurally related to AEA, does not bind CB<sub>1</sub> or CB<sub>2</sub> receptors and yet increases AEA-stimulated migration of BV-2 cells through a distinct receptor that couples to G<sub>i/o</sub> proteins<sup>72,91</sup>. Accordingly,

arachidonylcyclopropylamide (ACPA), a CB<sub>1</sub> agonist, regulates the migration of the mouse microglial cell line BV-2, but this response is not affected by SR1, emphasizing the distinct pharmacological profile of these uncharacterized receptors<sup>98</sup>. Evidence shows that such receptors are also expressed by astrocytomas. Specifically, THC, CP, and JWH-015 inhibit proliferation and promote apoptosis in the C6 rat glioma cell line, and this response is not blocked by CB antagonists<sup>99,100</sup>. Clearly, a large number of studies are required to increase our understanding, identity, and function of these receptors expressed by microglia and astrocytomas.

A number of receptors that have been identified at the molecular level and are phylogenetically distant from CB<sub>1</sub> and CB<sub>2</sub> receptors are also activated or antagonized by cannabinoids and cannabinoid-like compounds. A particularly well-studied example is GPR55, which shares little homology with CB<sub>1/2</sub> (13.5% and 14.4% respectively<sup>101</sup>). This receptor has recently been deorphanized with the discovery that LPI is its endogenous ligand, and it is antagonized by CBD<sup>102,103</sup>. To date, the precise pharmacological profile of GPR55 remains uncertain, as eCBs, phytocannabinoids, and synthetic cannabinoids bind this receptor and regulate cell signaling with varying potencies<sup>102,104–107</sup>. GPR55 is expressed in microglia and cancer cell lines, including GBM cell lines, regulates migration, proliferation and viability, and is an indicator of tumor severity<sup>105</sup>. There are several therapeutic opportunities for compounds that target this receptor as it has been implicated in immune cell activation<sup>108</sup> and shown to interact with CB<sub>2</sub> to regulate cytoskeletal reorganization and migration<sup>106</sup>.

GPR18 was originally discovered in testis and spleen and is currently thought to be what was referred to as “the putative abnormal-CBD (abn-CBD) receptor”<sup>93,109</sup>. A study pharmacologically profiling isolated human neutrophils pointed to the role of an abn-CBD receptor in modulating cell migration<sup>110</sup>. By using a combination of cannabinoid ligands, the authors concluded that this new receptor is distinct from CB<sub>1</sub> and GPR55 and that it may interact with CB<sub>2</sub> receptors. A follow-up study on BV-2 cell migration demonstrated that GPR18 is indeed activated by abn-CBD<sup>111</sup> and corroborated earlier findings that N-arachidonylglycine (NAGly) is an endogenous ligand<sup>112</sup>. NAGly is a metabolite of AEA that does not bind CB<sub>1</sub> and CB<sub>2</sub> receptors and yet, has profound anti-inflammatory and anti-nociceptive properties in rodent models<sup>113–115</sup>. These studies provide a strong foundation to medicinal chemists that are developing new generation of ligands that bind specifically to these targets and will ensure a high level of confidence in the pharmacological profile of their drugs.

## Novel targets for GBM therapeutics - the next line of treatment

TAMs make up as much as thirty percent of the entire GBM tumor mass<sup>49</sup> and play an active role in both the survival and progression of GBM tumors. TAMs secrete factors that promote angiogenesis and temper immune responses. Consequently, compounds that modulate TAM number and phenotype represent promising therapeutics to treat GBM tumors. As discussed above, cell migration is tightly controlled by both CB and CB-like receptors. Accordingly, compounds targeting these receptors would represent a distinct generation of therapeutics to indirectly affect GBM progression by blocking the cell migration of TAMs and reducing the amount of support that these cells provide to GBM cells. An alternative approach is based on taking advantage of TAMs as drug delivery shuttles that deliver therapeutics directly into the GBM tumor mass. A recent proof-of-concept study showed that a microglial cell line heterologously expressing thymidine kinase may serve as a vector or shuttle for gene therapy and can undergo apoptosis when gancyclovir is administered<sup>116,117</sup>. In line with these results, microglia may be labeled with gadolinium, a commonly used contrast agent in MRI, and used to image tumors. In fact, microglia can be packaged with both the thymidine kinase gene and gadolinium and used both as diagnostic tool and therapy<sup>118</sup>. These studies capitalize on the principal that TAMs are integrated as part of the tumor mass and should be destroyed along with the rest of the tumor. Thus both chemical and genetic approaches leading to a reduction or complete loss of TAMs will likely provide therapeutic benefit to GBM patients.

The need for novel therapies to treat GBMs remains unmet and urgent. Current chemotherapeutic options only lengthen the survival time of these patients by a few months and are associated with severe side effects that greatly reduce quality of life. Since patients potentially face a limited amount of time after diagnosis, an effective and efficient course of treatment is paramount following surgical debulking. As we discussed above, because of the presence of GCS, there is a high probability that the tumor will develop resistance to chemotherapy and radiation. This grim scenario emphasizes the need to tackle the disease from many directions: directly treating the remaining GBM and GCS cells, blocking angiogenesis, reestablishing BBB impermeability, and promoting an environment that stimulates cellular repair. The next generation of therapeutic approaches for treating GBM tumors will likely be based on set combinations of compounds designed to hit selective receptor targets to kill tumor cells based on their genetic fingerprint, and to modulate TAM migration and phenotype to halt tumor progression (see Figure 1). The accumulating evidence on the function of the eCB signaling system and CB-like receptors in the various cell types encompassed within GBM tumors point to a novel therapeutic avenue for the treatment of this type of cancer that can be pharmacologically enhanced to retain an optimal safety profile.

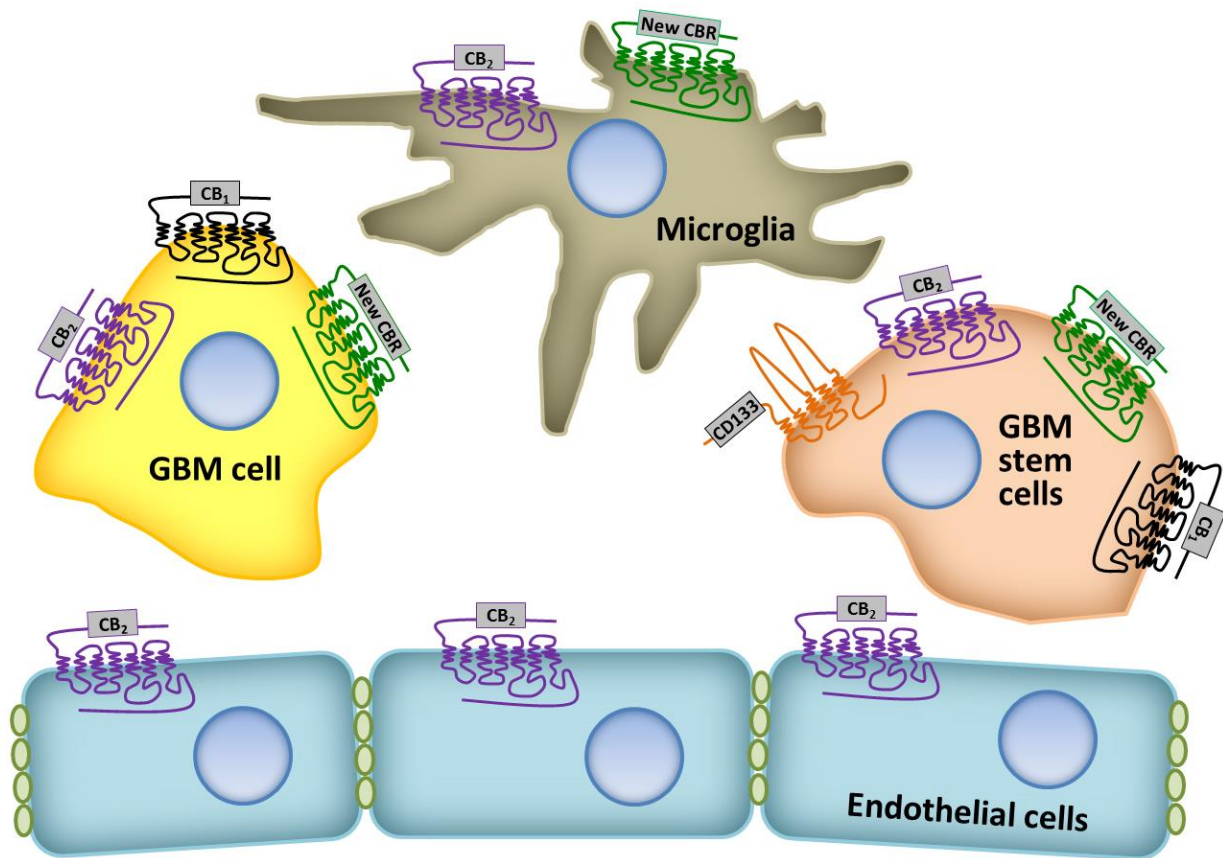


Figure 1: CB receptors expressed in the GBM tumor mass. Schematic of the composition of various cell types forming GBM tumors show that CB receptors can be targeted for the treatment of this disease. CB<sub>1</sub> and CB<sub>2</sub> receptors are expressed by microglia, GBM cells, GBM stem cells, and endothelial cells, and can be targeted to promote cell death in GBM and control inflammation by modulating the phenotype of microglia. New CB receptors may also be selectively targeted to promote these activities.

# CHAPTER 1: Alkylindole-sensitive receptors modulate microglial cell migration and proliferation

## Abstract

Ligands that target specific subtypes of G protein-coupled receptors (GPCR) expressed by microglia regulate distinct components of microglial cell activation. Thus, such agonists can regulate microglial cell proliferation, migration, and/or expression of effector proteins characteristic of the M1 or M2 phenotypes and represent promising therapeutics to treat brain diseases associated with microglial cell activation. Recent evidence has shown that microglia express alkylindoles (AI) receptors, a recently-identified class of cannabinoid-like receptors that couple to G proteins and are activated by AI analogues, but not by other classes of cannabinoid ligands. To date, detailed studies of AI receptor function in controlling microglial cell activation has been difficult as no selective pharmacological tools are available. Here, we used three newly-developed AI receptors ligands, ST-11, ST-47, and ST-48 to determine if microglia express functional AI receptors and to study how these novel targets regulate microglial cell activation. We found that primary mouse microglia express functional AI receptors by measuring radioligand binding and observing changes in intracellular cAMP levels, and that these receptors control both basal and ATP-stimulated cell migration. AI-receptor ligands inhibit cell proliferation stimulated by macrophage-colony stimulating factor (M-CSF) without effecting basal cell proliferation. Remarkably, these agonists do not control the expression level of select effector proteins characteristic of the M1 or M2 phenotypes. Our results suggest that microglia express functional AI receptors that control distinct components of the microglial cell activation process and that agonists at these novel targets might represent a promising approach for controlling microglia accumulation at lesion sites.

## Introduction

Microglia play a central role in the brain's response to various types of injuries, including injuries induced by changes in local metabolic supplies and homeostasis, infections and pathological processes<sup>56</sup>. The phenotype of microglia is generally accepted to be both highly plastic and tailored by the distinct panels of mediators that are produced under different types of brain injuries<sup>49,119</sup>. Thus, microglia express membrane receptors that sense the mediators associated with neuroinflammation, immune responses, and tissue

repair. The combined activation of distinct sets of membrane receptor subtypes expressed by microglia triggers diverse changes in their phenotype and cellular function and thus, tailors microglial response to various types of insults.

Among the different classes of membrane receptors expressed by microglia, G protein-coupled receptors (GPCR) have been shown to control distinct components of microglial cell activation. For example, purinergic P2Y<sub>12</sub> receptors are activated by ATP released from injured cells and control the extension and retraction amplitude of microglial cell processes “patrolling” the local parenchyma<sup>120–122</sup>. Cannabinoid CB<sub>2</sub> receptors are activated by endocannabinoids produced by cell injury and control multiple components of the microglia cell activation process, including cell proliferation, cell migration and the expression of characteristic M1 phenotype effector proteins such as pro-inflammatory cytokines and free radicals<sup>67,93,123,124</sup>. Additional examples of GPCR subtypes known to regulate distinct components of microglial cell activation, such as stimulated cell migration, include GPR55 and GPR18, which are activated by lysophosphatidylinositol and N-arachidonoyl glycine, respectively<sup>102,104,111,112,125</sup>. Some GPCR subtypes, such as mu opioid receptors, inhibit microglial cell chemotaxis induced by C5a, providing a feedback mechanism to fine-tune microglia cell migration<sup>126</sup>. Together, these studies indicate that the panels of mediators produced by each type of injuries will regulate the density and phenotype of activated microglia accumulating at lesion sites. Based on this evidence, GPCR expressed by microglia represent promising targets for therapeutics developed to modulate their activation process and the resulting course of the brain’s response to injury.

Recent evidence suggests that microglia express novel GPCR subtypes that remain uncharacterized with regard to their pharmacological profile, coupling mechanism and molecular identity<sup>73</sup>. Specifically, microglia express cannabinoid-like receptors activated by the prototypical AI agonist at CB<sub>1</sub>/CB<sub>2</sub> receptors, WIN55212-2, and not by the phytocannabinoid, <sup>9</sup>Δ-tetrahydrocannabinol (THC), or the AC-bicyclic analogue of THC, CP55940<sup>72</sup>. These receptors are commonly referred to as AI-sensitive receptors<sup>127</sup> and likely regulate microglial cell activation. Thus, ligands acting on these receptors might represent promising therapeutics to treat a variety of brain insults<sup>128,129</sup>. We recently developed new AI analogues that activate AI-sensitive receptors with nanomolar potencies, exhibit reduced affinity at CB<sub>1</sub>/CB<sub>2</sub> receptors and allow to study the coupling mechanism and biological role of these novel receptors in various model systems. Here, we sought to utilize these novel pharmacological tools to determine if AI-sensitive receptors are expressed by mouse microglia in primary culture and whether they control microglia cell activation.

## Results

### Microglia express functional AI-sensitive receptors

To determine if microglia express functional AI-sensitive receptors, we selected three AI analogues that contain chemical characteristics required for binding selectivity and receptor activation (Figure 1a-c) (manuscript in preparation). Specifically, ST-11 and ST-48 activate AI-sensitive receptors with nanomolar potency and contain a methyl moiety on the 2 position of the indole to reduce interaction with CB<sub>1</sub>/CB<sub>2</sub> receptors (Figure 1a,b)<sup>130</sup>. ST-11 represents the basic chemical scaffold used for designing the new series of AI analogues. ST-48 contains a morpholino moiety linked to the indole ring, which increases water solubility. We also selected one AI analogue (ST-47) that does not bind to AI-sensitive receptors despite minimal chemical difference and accordingly represents a useful selectivity control (Figure 1c). ST-47 contains a methoxybenzene moiety instead of a 4-methylnaphthoyl moiety that precludes binding to AI receptors. Thus, ST-11, ST-47, and ST-48 interrogate critical chemical characteristics required for binding to and activation of AI-sensitive receptors.

Two lines of evidence obtained by measuring [<sup>3</sup>H]WIN55212-2 radioligand binding in microglia membranes suggest the presence of AI-sensitive receptors and, as previously shown, the absence of CB<sub>1</sub>/CB<sub>2</sub> receptors (unless microglia are activated by select cytokines)<sup>63,120,131</sup>. First, WIN55212-2 competed for [<sup>3</sup>H]WIN55212-2 binding ( $k_i = 74$  nM), whereas the CB<sub>1</sub> antagonist O-2050 and CB<sub>2</sub> antagonist SR144528 (SR2) did not compete (Figure 1d,e). Second, ST-11 and ST-48 competed for [<sup>3</sup>H]WIN-55212-2 binding ( $k_i$  of 35 nM and 14 nM, respectively) while ST-47 did not compete (Figure 1d, e).

Several studies have suggested that AI-sensitive receptors couple to G proteins<sup>94,95</sup> (manuscript in preparation). Thus, we tested whether AI analogues control microglial cAMP levels as an index of GPCR coupling to G<sub>s</sub> and/or G<sub>i/o</sub> proteins. We treated microglia in primary culture with ST-11, ST-47 and ST-48 and measured changes in intracellular cAMP levels using a radioimmunoassay. We found that both ST-11 and ST-48 increased cAMP with maximal responses of 303 ± 81% and 206 ± 33% of basal levels, respectively (Figure 1f), and ST-47 produced no effect (Figure 1g). In support of an amplification mechanism mediated by GPCR coupling to effector proteins, the potency of these responses ( $EC_{50} = 2$  and 9.4 nM for ST-11 and ST-48, respectively) were achieved with lower concentration of ligands compared with their binding affinities (compare Figure 1d and 1f)<sup>132</sup>. These results suggest that AI-sensitive receptors couple to G<sub>s</sub>, although with somewhat low efficacy, since by comparison, the β-adrenergic receptor agonist isoproterenol increased microglial cAMP levels by an average 10-fold over basal. To rule out the involvement of G<sub>i/o</sub> proteins, we incubated microglia for 24

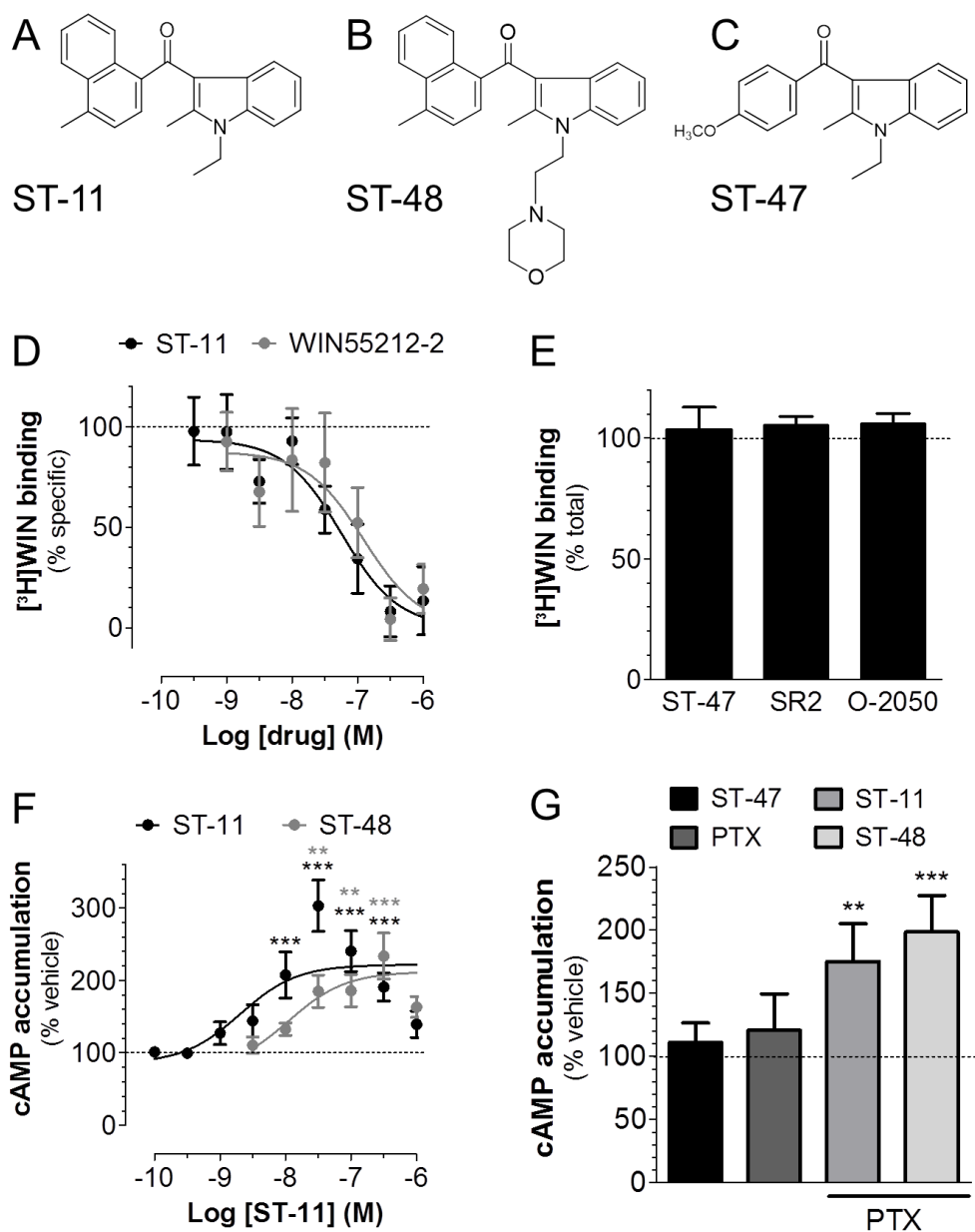


Figure 1: Microglia AI-sensitive receptors couple to  $G_s$  proteins. (A-C) Chemical structures of ST-11 (A), ST-47 (B), and ST-48 (C). (D) WIN5212-2 (WIN), ST-11 and ST-48 dose-dependent competition of [<sup>3</sup>H]WIN5212-2 binding in microglial membranes (WIN,  $n = 3-5$ ; ST-11,  $n = 4-6$ ; and ST-48,  $n = 3-4$ ). (E) ST-47 (1  $\mu\text{M}$ ) and cannabinoid ligands, SR2 (300 nM) and O-2050 (100 nM) do not compete for [<sup>3</sup>H]WIN5212-2 binding in microglial membranes (SR2,  $n = 4$ ; and O-2050 and ST-47,  $n = 3$ ). (F) ST-11 dose-dependently increases intracellular cAMP levels in primary cultured microglia (\*\* $P < 0.01$  and \*\*\* $P < 0.001$  compared with vehicle-treated cells,  $n = 3-8$  independent experiments, performed in triplicate). (G) PTX (1  $\mu\text{g/ml}$ ) does not block the ST-11 (300 nM) or ST-48 (1  $\mu\text{M}$ ) stimulated increase of cAMP levels (\* $P < 0.05$ , \*\* $P < 0.01$ , and \*\*\* $P < 0.001$  compared with vehicle-treated cells,  $n = 3$  independent experiments).

hrs with pertussis toxin (PTX) to uncouple  $G_{i/o}$  proteins and determined if this treatment affected the responses induced by ST-11 and ST-48. As expected, PTX incubation did not modify the ST-11- and ST-48-stimulated increase in cAMP levels suggesting that AI receptors couple to  $G_s$  proteins (Figure 1g). Together, these results show that mouse microglia in primary culture express functional AI-sensitive receptors and support previous studies reporting the absence or very low expression of  $CB_1/CB_2$  receptors in this model system<sup>63,120</sup>.

### AI-sensitive receptors control microglial cell migration and proliferation

GPCRs regulate distinct aspects of cell migration, including basal and stimulated migration<sup>133</sup>. Specifically, basal cell migration can be categorized as the random motility of the cell body occurring in the absence of a chemical stimulus. Stimulated migration encompasses two main mechanisms: chemokinesis, the increased random cell migration in response to a chemical stimulus, and chemotaxis, the stimulation-directed migration towards an increasing chemical gradient<sup>133,134</sup>. To determine whether AI-sensitive receptors regulate basal and/or stimulated cell migration, we tested if the prototypical AI analogue ST-11 alters basal and/or ATP-stimulated migration. Specifically, we measured cell migration by quantifying the number of cells labelled with a near infrared-emitting dye that had migrated to the bottom surface of a Boyden chamber filter (Figure 2a)<sup>120</sup>. ATP was chosen as a stimulus because it is released by injured cells and promotes both chemokinesis and chemotaxis in microglia<sup>122</sup>. We found that the low levels of basal cell migration were significantly inhibited by ST-11 ( $34 \pm 10\%$ ,  $n = 8$ ,  $P < 0.001$  compared with vehicle-treated cells) (Figure 2a). ATP increased migration by 2.9 fold over basal migration (Figure 2b), and ST-11 dose-dependently inhibited this response by  $46 \pm 9\%$  ( $IC_{50} = 868$  pM) (Figure 2c). To exclude the possibility that this inhibitory response was produced by acute cellular toxicity of ST-11, cell viability was assessed using the tetrazolium salt WST-1<sup>135</sup>. We found that ST-11 did not affect cell viability at concentrations up to  $3 \mu\text{M}$  (Figure 2d). These results suggest that AI receptors negatively modulate both basal and stimulated microglial cell migration.

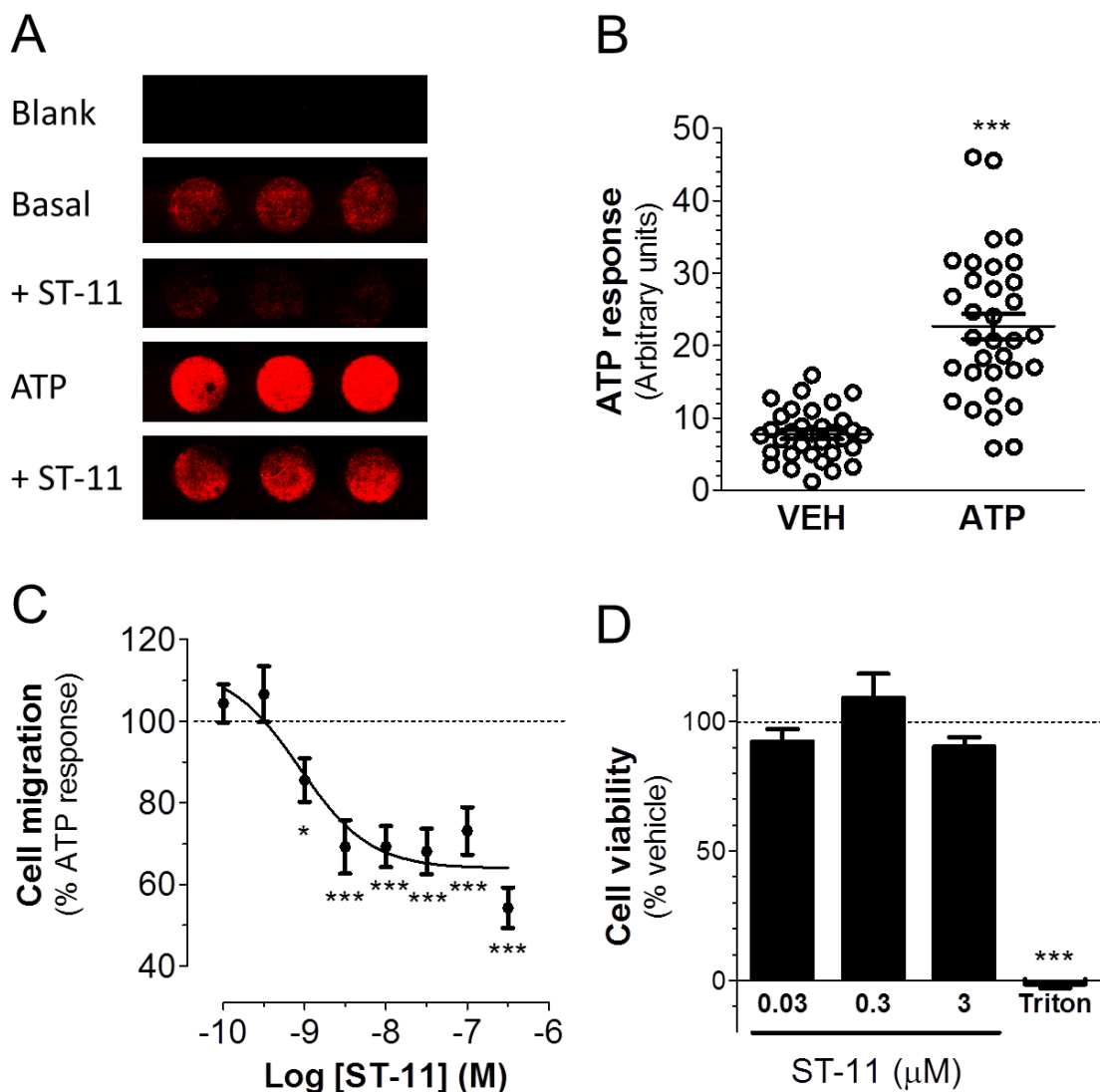


Figure 2: AI-sensitive receptors negatively modulate microglial cell migration. (A) Representative images of microglia that have migrated through a polycarbonate filter with 10- $\mu$ m pores. Background fluorescence was subtracted from all conditions tested and is represented by the blank image. This filter shows ST-11 treatment (300 nM) in the presence or absence of ATP (300  $\mu$ M). (B) ATP (300  $\mu$ M) stimulates primary microglia migration over basal migration (\*\* $P$  < 0.001 compared with vehicle-treated cells,  $n$  = 33 independent experiments performed in triplicate). (C) ST-11 dose-dependently inhibits ATP-stimulated migration (\* $P$  < 0.05, \*\* $P$  < 0.001 compared with vehicle-treated cells,  $n$  = 3-4 independent experiments performed in triplicate). (D) ST-11 does not cause cellular toxicity to primary microglia during a 3-hr period (\*\* $P$  < 0.001 compared with vehicle-treated cells,  $n$  = 3 independent experiments performed in triplicate).

Along with cell migration, mediators acting through GPCRs have been shown to increase and decrease cell proliferation depending on the receptor subtype<sup>123,136</sup>. To determine if AI-sensitive receptors regulate basal cell proliferation, we incubated mouse microglia in primary culture with [<sup>3</sup>H]thymidine and ST-11 for 72 hrs and measured the amount of [<sup>3</sup>H]thymidine incorporated into the cells by liquid scintillation. We found that ST-11 had no significant effect on basal proliferation (Figure 3a). To determine if AI receptors regulate stimulated cell proliferation, we incubated microglia with L929-conditioned media containing M-CSF, an agonist at CSF1R that triggers microglia cell proliferation and is produced in response to certain brain injuries<sup>137,138</sup>. M-CSF stimulated microglial cell proliferation by  $208 \pm 16\%$  ( $P < 0.001$  compared with vehicle treated cells; Figure 3b), and ST-11 decreased this response by 53% with an  $IC_{50}$  of 23 nM (Figure 3a). We verified that the decrease in proliferation was not due to cellular toxicity by concomitantly measuring cell viability with WST-1 and found no significant effect on cell viability (Figure 3c). These data suggest that AI-sensitive receptors do not affect the basal rate of cell proliferation yet inhibit cell proliferation stimulated by M-CSF.

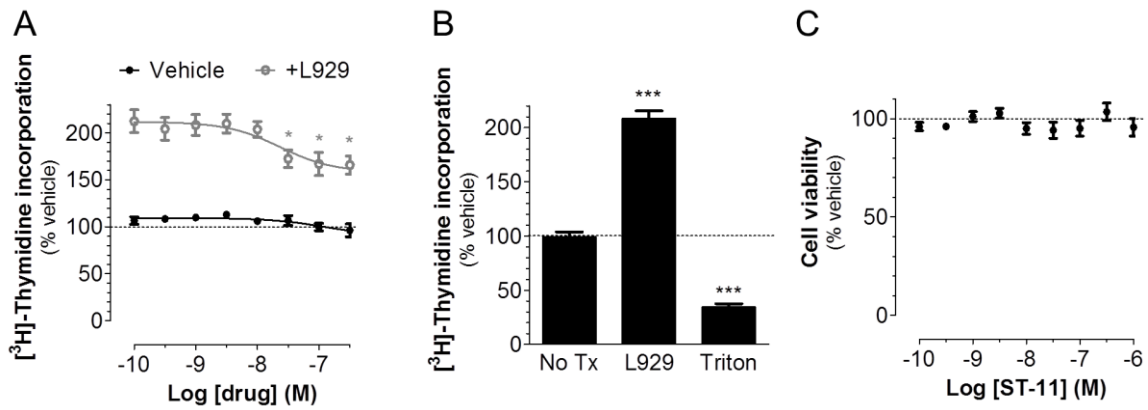


Figure 3: AI-sensitive receptor activation inhibits cell proliferation in primary microglial cells stimulated by M-CSF. (A) ST-11 does not affect basal cell proliferation but dose-dependently inhibits cell proliferation stimulated M-CSF (1% L929 condition media) (\* $P < 0.05$ ,  $n = 4-5$  independent experiments performed in triplicate). (B) 1% L929 added to cell culture media significantly increases cell proliferation (\*\*\*) $P < 0.001$  compared with 0.01% DMSO vehicle-treated cells,  $n = 6$  independent experiments performed in triplicate). (C) ST-11 does not affect microglial cell viability during 72 hrs ( $n = 3-8$  independent experiments performed in triplicate).

## AI receptors do not control microglial cell M1 and M2 phenotypes

An M1 phenotype is typified by the production of pro-inflammatory cytokines and free radicals and can be triggered by various stimuli, such as lipopolysaccharide (LPS) and IFN $\gamma$  + TNF $\alpha$ . The M2 phenotype is characterized by the up-regulation of Arginase 1, Chitinase-3-like protein 3 (Ym1), and Found in inflammatory zone 1 (FIZZ1) expression, which participate in tissue repair and can be triggered by IL-4. Several subtypes of GPCRs control microglial cell activation by modulating the key effector proteins that characterize the M1 and M2 phenotypes<sup>139</sup>. To determine if AI-sensitive receptors control the M1 phenotype, we incubated mouse microglia in culture with TNF $\alpha$  and IFN $\gamma$  and measured nitrite accumulation as an index of iNOS induction<sup>46</sup> and IP-10 accumulation as index of cytokine production<sup>140,141</sup>. We found that TNF $\alpha$ - and IFN $\gamma$ -stimulated microglia produced 4.2-fold more nitrites and 4.3-fold more IP-10 (Figure 4a-c). Remarkably, ST-11 did not affect either of these responses (Figure 4d-g). We next measured the effect of ST-11 on the M2 phenotype by incubating mouse microglia in culture with IL-4 and quantifying Ym1 and FIZZ1 mRNA expression by qRT-PCR<sup>142</sup> (Figure 5a,b). We found that IL-4 increased Ym1 and FIZZ1 mRNA expression and that ST-11 did not affect either basal or IL-4-stimulated Ym1 and FIZZ1 expression (Figure 5c). Together, these results suggest that AI-sensitive receptors do not control the expression of select M1 or M2 phenotype effector proteins.

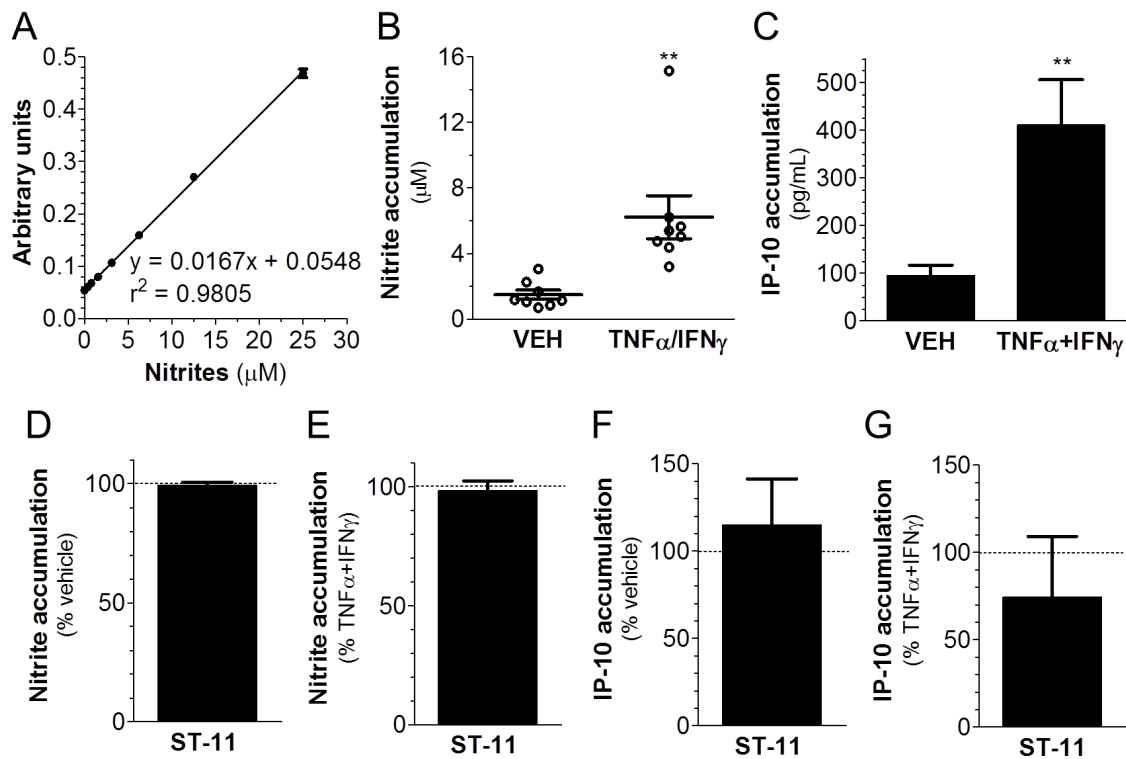


Figure 4: AI-sensitive receptors do not modulate the microglial M1 phenotype. (A) Nitrite accumulation measured based off of a calibration curve ( $n = 8$  independent experiments performed in triplicate). (B)  $\text{TNF}_\alpha$  and  $\text{IFN}_\gamma$  significantly increase nitrite levels (\*\* $P < 0.01$  compared with vehicle-treated cells,  $n = 8$  independent experiments performed in triplicate). Both the basal and  $\text{TNF}_\alpha/\text{IFN}_\gamma$ -stimulated increase in nitrate levels are within the linear range of the calibration curve (C)  $\text{TNF}_\alpha/\text{IFN}_\gamma$  treatment significantly increases IP-10 levels (\*\* $P < 0.01$  compared with vehicle treated cells,  $n = 3$  independent experiments performed in triplicate). (D, E) Nitrite levels measured under vehicle (D) or  $\text{TNF}_\alpha / \text{IFN}_\gamma$ -stimulated (E) conditions show no change when treated with ST-11 (300 nM) ( $n = 3$  independent experiments performed in triplicate). (F, G) Both IP-10 release under basal (vehicle-treated) (F) and stimulated with  $\text{TNF}_\alpha / \text{IFN}_\gamma$  (G) are not changed by ST-11 (1  $\mu\text{M}$ ) ( $n = 3$  independent experiments performed in triplicate).

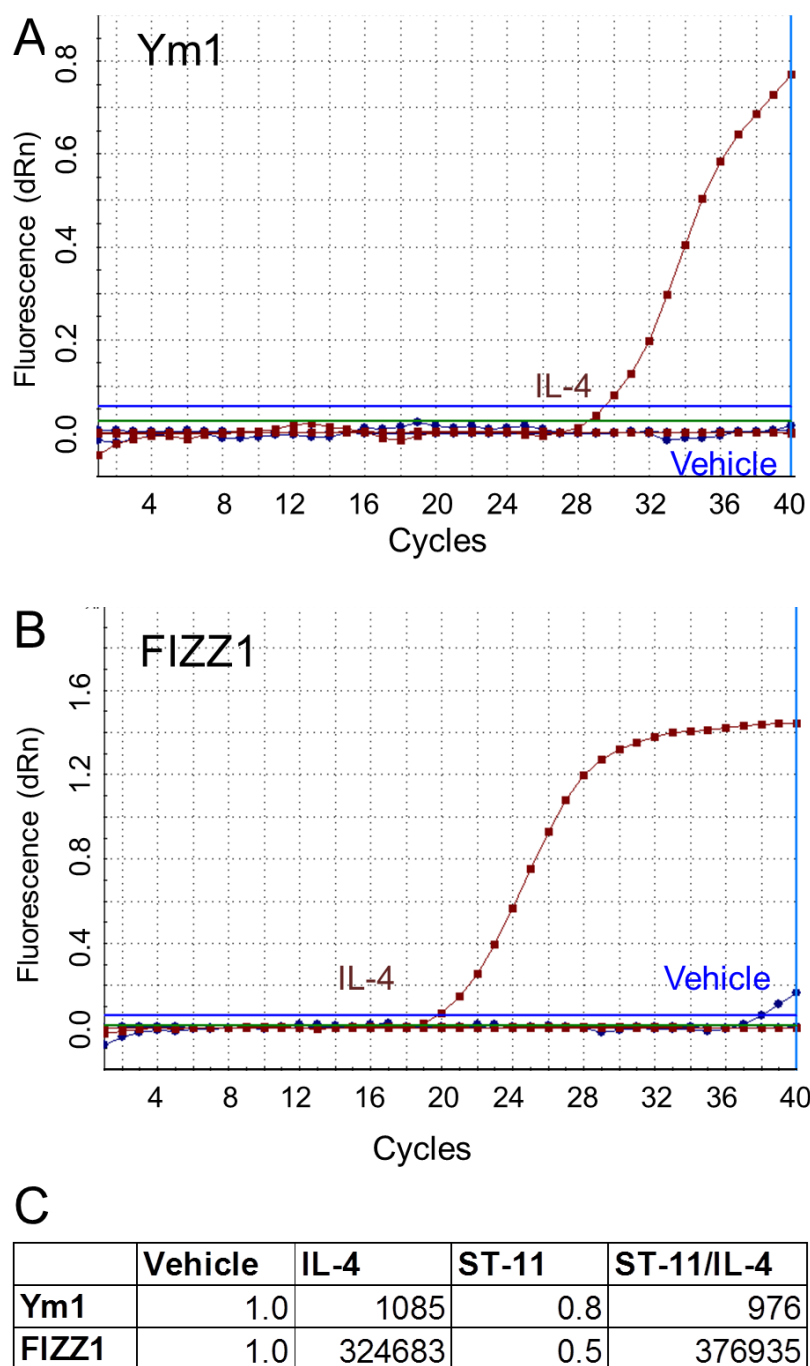


Figure 5: AI-sensitive receptors do not modulate the microglial M2 phenotype. (A,B) Representative  $C_t$  curves of the alternatively activated microglial Ym1 (A) and FIZZ1 (B) markers measured following treatment with vehicle or IL-4 (10 ng/mL). (C) The mRNA expression levels of Ym1 and FIZZ1 in microglia were not significantly changed by ST-11 (300 nM) ( $n = 3$  independent experiments performed in triplicate).

## Discussion

We found that microglial cells express functional AI-sensitive receptors that couple to G<sub>s</sub> proteins. Agonists acting at AI receptors reduce both basal and stimulated microglial cell migration suggesting that these novel receptors control both the random basal movement of microglia and their directed migration toward lesion sites. Agonists acting at AI-sensitive receptors do not affect basal cell proliferation but significantly reduce their stimulated cell proliferation, which suggests that AI-sensitive receptors do not directly control cell proliferation machinery but likely cross-talk with the signaling pathways triggered by M-CSF. Agonists acting at AI-sensitive receptors do not modulate the expression level of select effector proteins of M1 and M2 phenotypes, indicating that these GPCR control a subset of the molecular machinery involved in microglial cell activation.

Multiple studies suggest that microglia express novel cannabinoid-like receptors<sup>91,143,144</sup>. Whether these receptors were alkylindole-activated GPCRs (AI-sensitive receptors) or other unknown protein targets activated by cannabinoid-like ligands, including phycannabinoids and other synthetic cannabinoids, remained unclear. Specifically, conclusions regarding the involvement of a specific subtype of cannabinoid-like receptor were difficult to resolve because these studies used micromolar concentrations of cannabinoid agonists known to both activate CB<sub>1</sub>/CB<sub>2</sub> receptors with nanomolar potency and several off-target, unknown receptors and other protein targets. For example, micromolar concentrations of CP55940 and the AI analogue JWH-015 were required to decrease microglial NO production induced by IFN $\gamma$  and LPS<sup>65,69</sup>, cytokine production induced by LPS<sup>143,145</sup> and cell migration stimulated by ADP<sup>90</sup>, which raised the question of whether these effects were mediated through CB<sub>1</sub>/CB<sub>2</sub> receptors, AI-sensitive receptors or other unknown targets. The novel AI analogues used in our study exhibit nanomolar potencies at AI-sensitive receptors, reduced affinity at CB<sub>1</sub>/CB<sub>2</sub> receptors and allowed us to determine the components of microglia activation that are regulated by this novel subtype of GPCR.

Microglial cell migration can be triggered by an array of chemoattractants acting at GPCR, including peptides and proteins (e.g., chemokines), small hydrophilic molecules (e.g., nucleotides) and bioactive lipids (e.g. endocannabinoids)<sup>133,146,147</sup>. While stimulated microglial migration has been extensively studied, little data is available detailing the microglial cell migration “stop signal”, a response studied in more detail in other immune cell types, including T cells<sup>148</sup>. Such a “stop signal” may serve not only to instruct microglial cells to become less motile but may be used to guide microglial cell migration toward lesions by decreasing migration speed as the gradients of such signals increase closer to the injury site. Examples of GPCR subtypes that reduce cell migration

include CB<sub>2</sub> receptors stimulated by the HIV Tat protein<sup>149</sup>, mu opioid receptors stimulated by C5a<sup>126</sup>, and Y1 receptors stimulated by the pro-inflammatory cytokine IL-1β<sup>150</sup>. Our results indicate that agonists acting at AI-sensitive receptors reduce both basal and stimulated microglial cell migration, a result suggesting that the signaling network modulated by these GPCR likely exhibit direct control of the cell migration machinery.

Growth factors, such as M-CSF, increase cell proliferation by activating CSF1R and tyrosine kinase activity within the signaling network that controls cell proliferation<sup>137</sup>. Moreover, endocannabinoids acting on CB<sub>2</sub> receptors increases cell proliferation stimulated by CD40 activation or M-CSF and this response most likely involves a cross-talk between GPCRs and tyrosine kinase signaling<sup>123,136</sup>. Thus, while some studies suggest that some GPCR subtypes may control the initiation of cell proliferation, others, ours included, indicate that other GPCR subtypes modulate the effect of specific stimuli<sup>123,136,151</sup>. Indeed, a study has shown that a cannabinoid-like receptor inhibits basal proliferation of a microglial cell line<sup>152</sup>. Our study indicates that the signaling network controlled by AI-sensitive receptors likely cross-talks with signaling networks controlled by the tyrosine kinase receptor CSF1R.

In summary, we have shown that mouse microglia in culture express functional AI-sensitive receptors that control cell migration and stimulated proliferation. Accordingly, agonists activating through this novel target are likely to reduce the number of microglia migrating towards and accumulating at lesion sites, while not affecting their M1 or M2 phenotypes. Such compounds could be valuable to elucidate how reducing microglia cell number at lesion sites without affecting their phenotype might affect brain diseases associated with strong accumulation of microglial cells, such as has been demonstrated for malignant brain tumors and ischemic injuries<sup>153,154</sup>. Several important questions remain unanswered with regard to AI-sensitive receptors expressed by microglia. Among these unknowns are the molecular identity of these GPCR and their endogenous ligand(s), and whether other cell types in the brain and peripheral tissues express this target. Additional unknowns include the mechanism by which AI-sensitive receptors control the signaling network modulating microglia cell migration and proliferation and why they do not affect M1 or M2 phenotypes. The results obtained in our study provide a foundation for answering these questions. Based on the therapeutic potential of novel drugs capable of selectively controlling discrete components of microglial cell activation, our study clarifies the presence and role of AI-sensitive receptors in microglia, and provides initial evidence for the importance of further studying the therapeutic potential of targeting these GPCR to treat brain injuries.

## Acknowledgments

The authors would like to thank Drs. Gwenn Garden for helpful discussions and Thomas Möller for helpful discussions and help with IP-10 measurements, and Allison Cherry, Brian Haas, Eric Horne, and Alipi Naydenov from the Stella laboratory for help editing this manuscript. This work was funded by NIH (DA014486 to NS, DA007278 to SF).

## Materials and Methods

**Reagents:** ST-11 was synthesized by John W. Huffman at Clemson University, and ST-47 and ST-48 were synthesized by Medchem Source (Seattle, WA). SR144528 was provided by the NIDA drug supply program (RTI International, Research Triangle Park, NC). WIN55212-2 and O-2050 were purchased from Tocris (Minneapolis, MN), and ATP and isoproterenol were purchased from Sigma (St Louis, MO). [<sup>3</sup>H]WIN55212-2 and [<sup>3</sup>H]thymidine were purchased from Perkin Elmer (Boston, MA).

**Cell culture and migration:** All experiments were performed in accordance with Institutional Animal Care and Use Committee at the University of Washington. Primary cultures of mouse microglial cells were generated from 1-3 days old C57BL-6 pups as previously described<sup>155</sup>. Briefly, mixed glial cell cultures were maintained in T75 flasks (BD Biosciences, San Jose, CA) in DMEM supplemented with 10% FBS, 10% F12 media, 5 mM HEPES, 100 UI penicillin and 100 µg/ml streptomycin up to six weeks. Starting on week two and every week thereafter, floating and loosely adherent microglia were harvested by shaking. Cells were used in Boyden chamber migration assays as previously described with minor modifications<sup>120</sup>. Specifically, filters with a pore diameter of 10 µm (Neuroprobe, Gaithersburg, MD) were incubated in 10 ml of a collagen solution (2.5 mg rat tail collagen I (BD Biosciences, San Jose, CA), 57 µl glacial acetic acid (Fisher, Santa Clara, CA) in 50 ml distilled water) for 30 min at 37°C. Filters were rinsed 3 times with PBS and allowed to dry before use. Following a 3 hrs migration period at 37°C, the number of NIR-labelled cells was quantified using the Odyssey Infrared Imaging System (LI-COR, Lincoln, NE) and the following scanning settings: resolution, 169 µm; quality, low; focus off-set, 1 mm; and intensity, 4.0.

**Radioligand binding:** Microglia membranes were prepared by lysing cells with ice-cold homogenization buffer composed of the following: Tris (50 mM), EDTA (1 mM), and MgCl<sub>2</sub> (3 mM). Lysed cells were homogenized with a Dounce homogenizer (Wheaton Science Products, Millville, NJ). Homogenates were centrifuged at 200 x g for 10 min at 4°C, and the supernatant was collected and stored at -80°C until further use. On the day of experiments, membranes were thawed and pooled, and the protein concentration was quantified with the DC protein assay (BioRad, Hercules, CA) using BSA as a

standard. All experiments were performed using silanized glass test tubes (Alltech, Deerfield, IL) and silanized pipette tips (VWR Scientific, Brisbane, CA) to minimize the loss of hydrophobic compounds. Binding buffer (pH 7.4) contained the following: Tris-base (50 mM), EDTA (1 mM), MgCl<sub>2</sub> (3 mM), and BSA (1 mg/ml). The following components were added to test tubes placed on ice: 50 µl of binding buffer with compound, 50 µl of binding buffer with radioligand, and 100 µl of binding buffer containing membranes (100 µg of protein). Tubes were then covered and incubated for 1 hr in a 30°C-water bath with mild agitation. Reactions were stopped by rapid filtration using a Brandel harvester (Brandel, Gaithersburg, MD), collecting radioactive membranes on Whatman GFB filter strips (Brandel, Gaithersburg MD), and rinsing with ice-cold binding buffer. Filters were transferred to 7-ml glass scintillation vials (VWR Scientific, Brisbane, CA) using the Brandel Manual Deposit System (Brandel, Gaithersburg, MD), and 4 ml scintillation fluid (National Diagnostics, Atlanta GA; Ecoscint XR) was added to each scintillation vial. Samples were vortexed for 10 sec and followed by 18 hrs incubation at room temperature prior to quantifying radioactivity with a scintillation counter (PerkinElmer, Boston, MA).

cAMP measurement: cAMP levels were measured as previously described<sup>91</sup>. Briefly, microglia were seeded at  $5 \times 10^4$  cells per well in 48-well plates (Corning, Tewksbury, MA) and maintained for 24 hrs in the cell culture conditions described above. When required, PTX (1 µg/ml) was added to the culture media 24 hrs after cell seeding. To measure cAMP levels, cells were placed in a shaking water bath at 37°C with mild agitation, and culture media were replaced with 500 µl of assay buffer: composed of the following: HEPES (20 mM), NaHCO<sub>3</sub> (5 mM), NaCl (100 mM), KCl (5 mM), CaCl<sub>2</sub> (2 mM), MgSO<sub>4</sub> (1 mM), NaH<sub>2</sub>PO<sub>4</sub> (1 mM), and D-(+)-glucose (10 mM). After 15 min, the buffer was replaced by a pre-incubation buffer containing non-specific phosphodiesterase inhibitor IBMX (1 mM), and after 10 min, this buffer was replaced with buffer containing both IBMX and the indicated ST-compounds for 15 min at 37°C. The reaction was stopped by the addition of 75 µl of 0.1% Triton X-100 in NaOH (0.1 M) and 75 µL of 0.1% Triton X-100 in HCl (0.1 M). Sample lysates were used to quantify cAMP levels using a [<sup>125</sup>I]cAMP radioimmunoassay kit according to the manufacturer's guidelines (PerkinElmer, Waltham, MA).

Cell viability and proliferation: Microglia were plated at a density of  $2.5 \times 10^4$  cells/well in 48-well plates (Corning, Tewksbury, MA) and maintained in normal cell culture conditions for 24 hrs. Cells were treated with ST-compounds and [<sup>3</sup>H]thymidine (PerkinElmer, Waltham, MA) for 72 hrs at 37°C. To measure cell viability concomitantly with cell proliferation, cells were incubated with 10 µl WST-1 (Roche, Indianapolis, IN) 60 min before cell lysis and returned to 37°C. The WST-1 absorbance was measured using a SpectraCount BS10000 (PerkinElmer, Waltham, MA.) at a wavelength of 450 nm. Culture media was removed, and cells were rinsed with 250 µl ice-cold PBS and lysed with 250 µl NaOH (1 M). Cell lysates were kept on ice for 10 min and then

transferred to 7-ml glass scintillation vials (VWR Scientific, Brisbane, CA). Distilled H<sub>2</sub>O (250 µl) was added to each vial followed by 4 ml scintillation fluid (National Diagnostics, Atlanta GA; Ecoscint XR). Samples were vortexed and radioactivity was measured using a scintillation counter (PerkinElmer, Waltham, MA).

Nitric Oxide and IP-10 measurements: Microglial were plated at a density of  $2 \times 10^5$  cells/well in 24-well plates (Corning, Tewksbury, MA) and maintained in standard cell culture conditions for 24 hrs. Culture media was switched to MEM supplemented with 10% Cellgro, 5 mM HEPES, 100 UI penicillin and 100 µg/ml streptomycin. Cells were pre-incubated with ST-11 for 24 hrs before treatment with TNF $\alpha$  (5 ng/ml) and IFN $\gamma$  (30 IU) (R&D Systems, Minneapolis, MN) for 24 hrs. Culture media (100 µl) was removed from each well and combined with 100 µl Griess reagent to measure nitrite levels by absorbance at 540 nm. The remaining culture media was removed and saved at -80°C for cytokine measurements. Cytokines were measured via a Luminex multiplex assay according to the manufacturer's instructions (Luminex, Austin, TX).

Quantitative RT-PCR: Microglia were plated at a density of  $5 \times 10^5$  cells/well in 6-well culture plates (Corning, Tewksbury, MA) and maintained in standard cell culture conditions for 24 hrs. Cells were switched to macrophage-serum free media (Life Technologies, Grand Island, NY) for 24 hrs, and ST-11 pre-treatment occurred for 1 hr before the end of the serum deprivation period. Cells were rinsed and returned to standard cell culture media and treated with IL-4 (10 ng/ml) (R&D Systems, Minneapolis, MN) or vehicle. Twenty-four hours later, cells were rinsed with PBS and frozen at -80°C until further use. RNA was isolated using a PerfectPure RNA Cultured Cell kit according to the manufacturer's instructions (5 PRIME, Gaithersburg, MD). The quantitative RT-PCR kit used was the LightCycler® 480 RNA Master Hydrolysis Probes (Roche, Indianapolis, IN) using the following primers: FIZZ1 (probe 3) forward, tatgaacagatgggctctct and reverse, aggcagttgcaagtatctcca; Ym1 (probe 88) forward, aagaacactgagctaaaaactctct and reverse, gagaccatggcactgaacg; Ribosomal protein S5 (probe 71) forward, cactgcgtcgagtgaatcag and reverse, gctcatctgcaaggcactc; Eukaryotic translation initiation factor 4A2 (probe 53) forward, cgatctacctaccaatcgtgaa and reverse, accttctcccaaactcgac; Ubiquitin C (probe 11) forward, gaccagcagaggctgatctt and reverse, cctctgaggcgaaggactaa.

Statistics: Prism software version 5.01 was used to conduct statistical analysis. Data are presented as mean  $\pm$  S.E.M., and statistical significance was determined with a one-way ANOVA followed by a post-hoc Dunnett's multiple comparison test or a two-tailed t-test.

## CHAPTER 2: In vivo evidence that alkylindole compounds promote apoptosis in astrocytomas independently of CB<sub>1</sub> and CB<sub>2</sub> receptors

### Abstract

Alkylindoles (AI) bind to and activate several protein targets, including the cannabinoid CB<sub>1</sub> and CB<sub>2</sub> receptors, and the AI-sensitive receptors that remain uncharacterized with regard to their molecular identity, pharmacological profile and coupling mechanism. Evidence shows that AI represent promising new anti-cancer drugs as they induce apoptosis selectively in tumor cells, including in astrocytomas. Whether the anti-tumor effects of AI occurs through CB<sub>1</sub>, CB<sub>2</sub> or AI-sensitive receptors has been difficult to resolve because of the absence of selective ligands for AI-sensitive versus CB<sub>1</sub> and CB<sub>2</sub> receptors. Here we investigated the therapeutic value and mechanism of action of a novel AI compound, ST-11, that exhibits nanomolar potency at AI-sensitive receptors and does not interact with CB<sub>1</sub> and CB<sub>2</sub>. ST-11 binds to AI-sensitive receptors expressed by the mouse astrocytoma cell line, DBT, and reduces cell migration and proliferation, and induces apoptosis. In vivo, ST-11 induces dose-dependent activation of apoptosis in DBT tumors implanted in mouse brain leading to tumor volume reduction and microglial cell activation, without inducing overt side effects. Our data show that AI analogues targeting AI-sensitive receptors represent a new class of anti-tumor compounds that exhibit a promising therapeutic index and act through a novel mechanism of action.

### Introduction

Astrocytomas are the most common primary brain tumors diagnosed in young and adult brains, and they are graded by the WHO to correspond with increases in malignancy and poorer prognosis. Thus, over 10,000 new patients are diagnosed with each year with grade IV astrocytoma (also known as glioblastoma multiforme) and the prognosis for these patients treated with standard of care is 17 months with 95% of patients dying within 5 years of diagnosis<sup>156</sup>. These dramatic numbers advocate for the development of new therapeutic approaches that will treat and hopefully cure this devastating type of cancer. Ideally, novel therapeutics would kill astrocytomas and reduce the severity of side effects. Evidence accumulated over several decades of research show that several classes of cannabinoid compounds carry these characteristics, as they selectively

promote apoptosis in malignant cells without affecting the viability of healthy cells or producing overt side effects<sup>80</sup>. As such, cannabinoid compounds represent a promising new class of anti-cancer drugs for the treatment of astrocytomas.

A wide range of biological effects produced by cannabinoid compounds are mediated via two cannabinoid receptors, CB<sub>1</sub> and CB<sub>2</sub>, yet recent evidence shows that a portion of the therapeutic properties carried by these compounds act through other targets. Over 40 years of medicinal chemistry led to the development of distinct classes of synthetic cannabinoid agonists based on distinct chemical scaffolds that exhibit nanomolar potencies at CB<sub>1</sub> and CB<sub>2</sub> receptors<sup>127</sup>. One such scaffold that has been extensively explored for its ability to interact with CB<sub>1</sub> and CB<sub>2</sub> receptors is AI<sup>130</sup>. The prototypical AI compound, WIN55212-2 (WIN-2), exhibits nanomolar potency at both CB<sub>1</sub> and CB<sub>2</sub> receptors and is often used to test for the involvement of these receptors in regulating various cell functions. Starting in the 1990s, several laboratories reported that WIN-2 lacks pharmacological selectivity at cannabinoid receptors and regulates distinct cell functions and signaling pathways independently of CB<sub>1</sub> and CB<sub>2</sub> receptors, suggesting the existence of novel protein targets that remain unidentified at the molecular level<sup>73</sup>. These receptors are commonly referred to as AI-sensitive receptors and evidence suggests that they can control astrocytoma pathogenesis. Specifically, the AI compound, JWH-015, inhibits C6 glioma cell division both in vitro and in vivo, and yet the pharmacological profile of these effects does not correspond to the known pharmacology of JWH-015 at CB<sub>1</sub> and CB<sub>2</sub> receptors<sup>100,157</sup>. To date, there are more than a dozen reports on the existence of AI-sensitive receptors in astrocytomas and yet few pharmacological tools are available to study this therapeutic target<sup>73</sup>.

We recently developed a novel series of AI analogues as first generation selective ligands for AI-sensitive receptors (unpublished data). Here we sought to use these novel pharmacological tools to determine if DBT cells, a mouse astrocytoma cell line known to lack CB<sub>1</sub> and CB<sub>2</sub> receptors<sup>83</sup>, express functional AI-sensitive receptors and whether activation of this novel target regulates key cell functions linked to astrocytoma pathogenesis, including cell migration, proliferation and viability. We also tested the therapeutic index of ST-11 by examining the in vivo safety profile and efficacy in a syngeneic mouse model of astrocytoma.

## Results

The mouse astrocytoma cell line, DBT, expresses AI-sensitive receptors and lack CB<sub>1</sub> and CB<sub>2</sub> receptors.

The six novel AI compounds that were selected for this study (ST-11, ST-23, ST-25, ST-29, ST-47 and ST-48) contain critical chemical modifications within the indole ring that dictate their binding affinities at AI-sensitive versus CB<sub>1</sub>/CB<sub>2</sub> receptors (Figure 1a-b and supplementary figure 1). Specifically, ST-11 represents the basic chemical scaffold used to design the novel series of AI compounds and contains a methyl moiety on the C2 position of the indole known to reduce interaction with cannabinoid receptors (Figure 1a)<sup>130</sup>. ST-23, ST-25, ST-29 and ST-48 bind to AI-sensitive receptors with nanomolar affinity and contain structural differences at both the C-2 and N-1 positions of their indole that differentially affect their affinity at AI-sensitive and cannabinoid receptors, and thus can be leveraged to further optimize selectivity (supplementary figure 1). ST-47 represents a useful selectivity control as it does not bind to AI-sensitive receptors despite minimal chemical difference (a methoxybenzene moiety instead of a 4-methylnaphthoyl moiety) (supplementary figure 1).

We tested whether these novel AI compounds and control cannabinoid compounds compete for [<sup>3</sup>H]WIN55212-2 binding, we determined if the DBT mouse astrocytoma cell line expresses AI-sensitive, CB<sub>1</sub> and CB<sub>2</sub> receptors and found three sets of evidence indicating that DBT cells express AI-sensitive receptors and lack CB<sub>1</sub> and CB<sub>2</sub> receptors. First, the non-selective compound WIN55212-2 competes for [<sup>3</sup>H]WIN55212-2 binding to DBT membranes ( $k_i = 66.6$  nM) (Figure 1c), whereas the selective CB<sub>1</sub>/CB<sub>2</sub> agonist CP55940, CB<sub>1</sub> antagonist SR141617 and CB<sub>2</sub> antagonist SR144528 did not compete for binding (supplementary figure 1e). Second, the prototypical AI compound, ST-11, competed for [<sup>3</sup>H]WIN55212-2 binding with a  $k_i$  of 18.5 nM and the inactive AI compound, ST-47, did not compete for binding (supplementary figure 1e). Third, ST-23, ST-25, ST-29 and ST-48 competed for [<sup>3</sup>H]WIN55212-2 binding with decreasing affinity and in the same rank order as measured for human AI-sensitive receptors ( $k_i = 40.4$  nM, 20.9 nM, 4.1  $\mu$ M, and 7.9 nM respectively, Figure 1c and data not shown). Using a saturating concentration of ST-11 (3  $\mu$ M), we found that [<sup>3</sup>H]WIN55212-2 binds to AI-sensitive receptor with a  $k_d$  of 6.2 nM and the DBT cells express significant amount of AI-sensitive receptors ( $B_{max}$  of 248.7 fmol/mg) (supplementary figure 1f). Together, these results indicate that the prototypical AI compound ST-11 exhibits nanomolar affinity at mouse AI-sensitive receptors and does not significantly activate mCB<sub>1</sub> and mCB<sub>2</sub> receptors, providing powerful pharmacological tools to study the function of AI-sensitive receptors in various model system, including DBT cells.

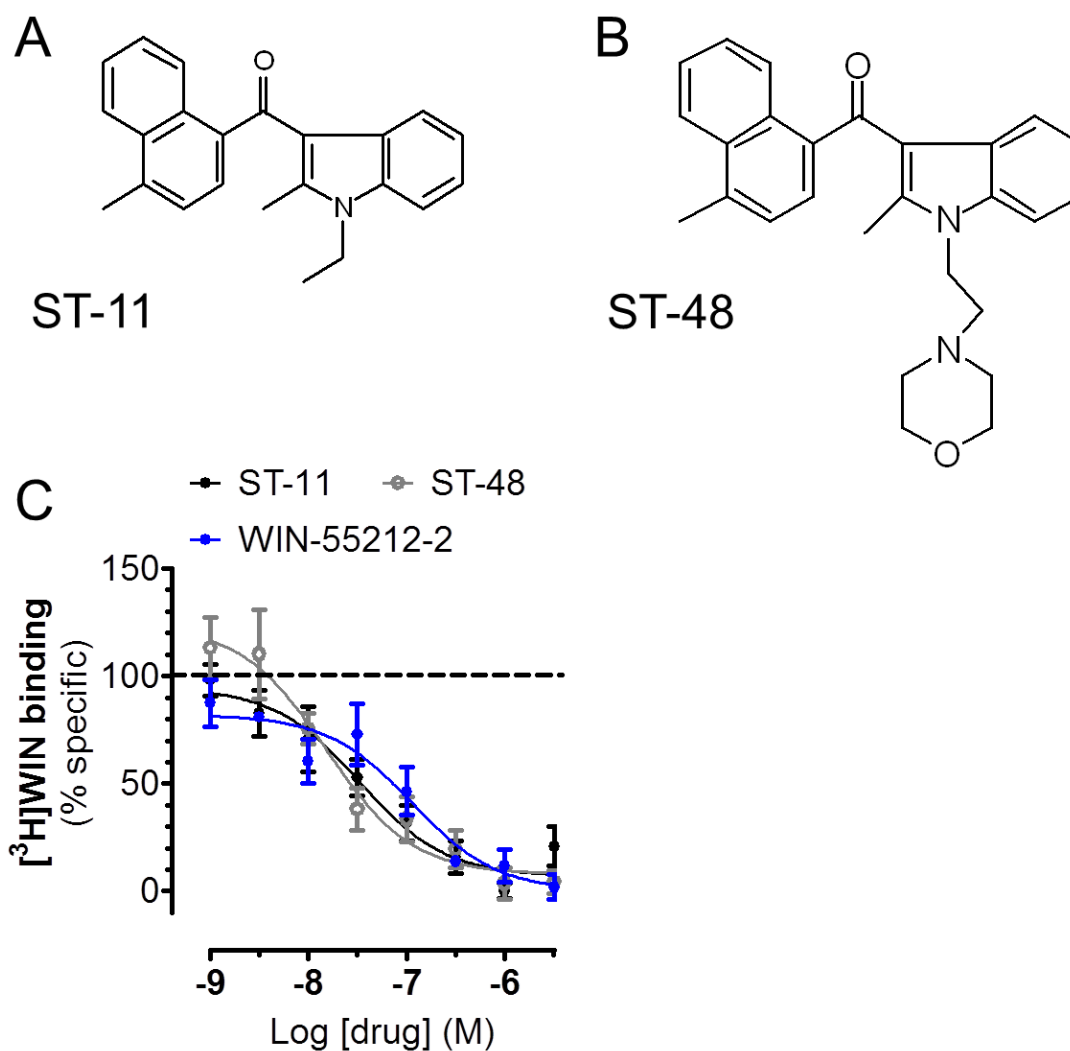
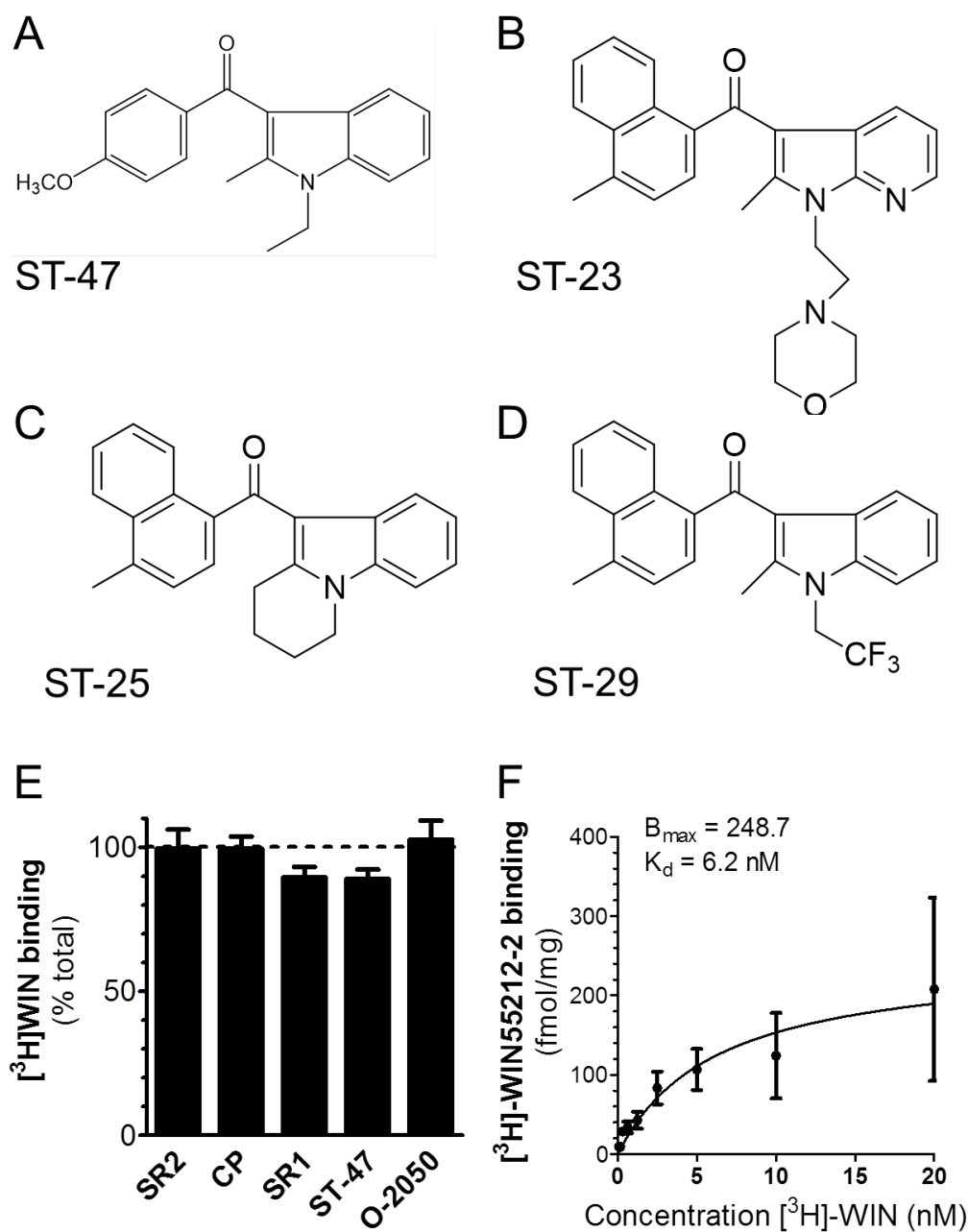


Figure 1: AI-sensitive receptors in astrocytoma cells are activated by ST compounds. (A-B) Chemical structures of (A) ST-11 and (B) ST-48. (C) WIN55212-2 (WIN), ST-11 and ST-48 dose-dependent competition of [<sup>3</sup>H]WIN55212-2 binding in DBT membranes (WIN and ST-11, n = 3-5; ST-48, n = 4 independent experiments, in triplicate). (D) Saturation binding data showing one binding site for WIN55212-2 (n = 4-5 independent experiments, in triplicate). (E) Competition binding of cannabinoid ligands SR2 (300 nM), CP (3 nM), SR1 (30 nM), O-2050 (100 nM), and inactive AI ST-47 (1 μM) showing minimal displacement of [<sup>3</sup>H]WIN55212-2.



Supplementary Figure 1: AI-sensitive receptors in astrocytoma cells do not bind cannabinoid compounds. (A-D) Chemical structures of (A) ST-47, (B) ST-23, (C) ST-25, and (D) ST-29. (E) Competition binding of cannabinoid ligands SR2 (300 nM), CP (3 nM), SR1 (30 nM), O-2050 (100 nM), and inactive AI ST-47 (1  $\mu$ M) showing minimal displacement of [<sup>3</sup>H]WIN55212-2. (n = 3 independent experiments, in triplicate). (F) Saturation binding data showing one binding site for WIN55212-2 (n = 4-5 independent experiments, in triplicate).

## AI receptors control cell migration, proliferation, and viability

To determine if activation of AI-sensitive receptors expressed by DBT cells will affect the growth of these tumor cells, we investigated whether ST-11 regulates DBT cell migration, proliferation and viability. To measure cell migration, we quantified the number of DBT cells that migrated toward the bottom surface of a Boyden chamber filter using a near infrared-emitting dye <sup>120</sup>. Migration was stimulated with 300 nM LPA by 5.1 fold over basal migration (Figure 2a). ST-11 and ST-48 dose-dependently inhibited this response (IC<sub>50</sub> = 56 nM, 3 nM respectively) (Figure 2b). To determine if AI-sensitive receptors control cell proliferation, DBT cells were treated with ST-11 and [<sup>3</sup>H]thymidine for 72 hrs, and thymidine incorporation was quantified by liquid scintillation. We found that ST-11 reduced thymidine incorporation by 58.3% ± 2.9% SEM, n=3 independent experiments) with an IC<sub>50</sub> of 1.1 μM (Figure 3a). We concomitantly examined if ST compounds negatively affected cell viability by measuring when treating the cells for 72 hrs (Figure 3b). ST-11 induced a dose-dependent decrease in DBT cell viability. Remarkably, ST-11 treatment of mouse neurons in primary culture did not affect their viability, thus providing initial evidence for a promising therapeutic effect of this analogue. Several reports suggest that AI analogues kill astrocytomas by inducing apoptosis. To explore this possibility, we treated DBT cells in culture with ST-11 and visualized caspase 3 activation by ICC. We found that ST-11 promoted apoptosis as indicated by a clear increase in the amount of cleaved caspase 3 in DBT cells after treatment with ST-11 for 2 hrs (Figure 3c). Note that cells with elevated levels of active caspase 3 also exhibited a condensed nucleus and a rounded cell body compared to vehicle-treated controls (Figure 3c inset). Together, these results suggest that DBT cells express functional AI-sensitive receptors that control key components of GBM pathogenesis, including cell migration, proliferation, and viability by promoting apoptosis.

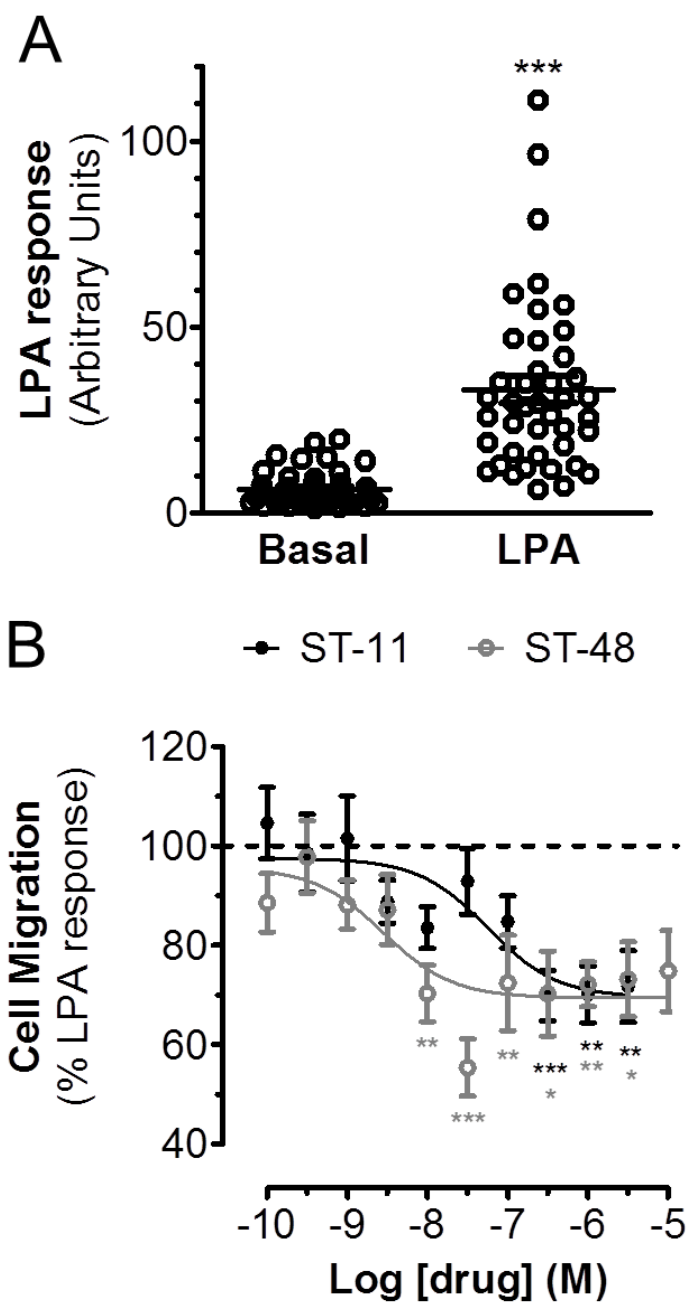


Figure 2: AI-sensitive receptors negatively modulate cell migration in astrocytoma cells. (A) LPA (300 nM) stimulates migration in DBT cells (\*\* $P < 0.001$  compared with vehicle-treated cells,  $n = 42$  independent experiments performed in triplicate). (B) ST-11 and ST-48 dose-dependently inhibit LPA-stimulated migration (\* $P < 0.05$ , \*\* $P < 0.01$ , \*\*\* $P < 0.001$  compared with vehicle-treated cells, ST-11 and ST-48,  $n = 3-5$  independent experiments performed in triplicate).

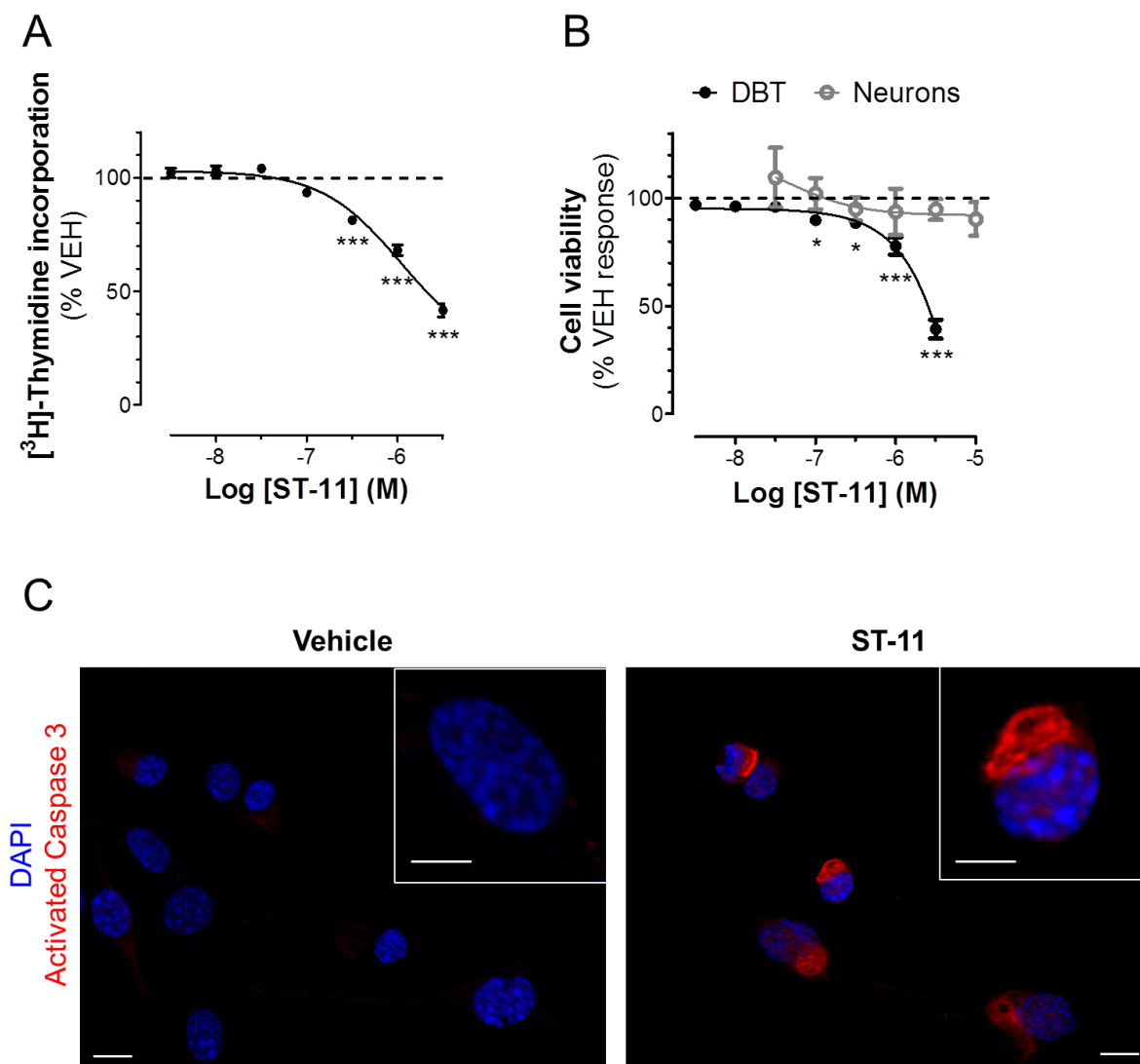


Figure 3: AI-sensitive receptor activation inhibits proliferation and reduces viability in astrocytoma cells. (A) ST-11 reduces basal cell proliferation ( $***P < 0.001$ ,  $n = 3$  independent experiments performed in triplicate). (B) ST-11 inhibits DBT cell viability within 72 hrs. By comparison, primary neurons treated with ST-11 for the same period are unharmed ( $*P < 0.05$ ,  $***P < 0.001$ , DBT,  $n = 3-4$ ; neurons,  $n = 3$  independent experiments performed in triplicate). (C) Caspase 3 activation is apparent in DBT cells treated with ST-11 (10  $\mu\text{M}$ ) within 2 hrs and absent in vehicle-treated cells.

## Solubility, pharmacokinetic profile, and safety of ST-11

Based on the pharmacological profile of ST-11, which includes nanomolar potency at AI-sensitive receptors and a lack of activity at CB<sub>1</sub> and CB<sub>2</sub> receptors, we selected this prototypical compound to test its safety and pharmacokinetic (PK) profile in mice. Our first goal was to test different formulations to ascertain solubility and stability of the drug. We found that ST-11 was less soluble compared to WIN-2 and that it was stable for only 24 hrs at 4°C in Cremophor® RH 40, ethanol, and saline (1:1:18), the most common formulation used for AI compounds (supplementary table 1). To circumvent this limitation, we explored formulations composed of combinations of lipids that form semi-solid nanospheres or liposomes. Liposomes are currently being used as FDA-approved drug delivery vehicles in humans for different diseases, including cancer, and represent an efficacious and non-toxic delivery system<sup>158,159</sup>. Our results suggest that liposomes represent a viable formulation approach that maintains ST-11 stability for at least 2 weeks.

Using this liposome formulation, we determined the maximal tolerated dose (MTD) of ST-11 injected to mice acutely and under a semi-chronic regimen (daily injections for 5 days). Thus mice were treated with ST-11 formulated at 5 mg/ml in liposomes using escalating doses up to 240 mg/kg administered via intraperitoneal (i.p.) injection either once or daily for 5 days, and signs of toxicity or distress were monitored (see materials and methods). Remarkably, we did not observe any adverse effects, including cannabimimetic symptoms, when administering up to 240 mg/kg daily over 5 days, indicating that the maximal administrable dose of ST-11 at 240 mg/kg remains well-tolerated. Because regimented use of AI compounds has been associated with tissue toxicity<sup>160,161</sup>, we harvested six principal organs (heart, liver, kidney, lungs, spleen and brain) from mice in the semi-chronic study and used an H&E stain to assess organ toxicity. We found no sign of toxicity in these organs when surveying tissue treated with ST-11 at 240 mg/kg. We did find that the highest volume of liposomes administered and the corresponding highest dose of ST-11 (240 mg/kg), both of which represent 1.2 ml injections per mouse, produced a small lymphoid hyperplasia in the marginal zone in the spleen. These results suggest a high rate of liposome phagocytosis linked to the large amounts of liposomes administered under both these conditions and independent of ST-11 (data not shown).

	WIN		ST11	
	<i>Day 1</i>	<i>Day 14</i>	<i>Day 1</i>	<i>Day 14</i>
30% mouse serum				
10% EtOH				
1% DMSO				
1% Tween-80				
2% Tween-80				
EtOH:Cre:Sal (1:1:18)				
1% Tween-80 + 10% FBS				

Key

	remained in solution
	precipitated
	partially dissolved

Supplementary Table 1: Solubility of WIN-2 and ST-11 in various formulations after 2 weeks.

To study the PK profile of ST-11 in mouse blood and brain, first we developed and validated an LC-MS method that quantifies ST-11 amounts in biological matrices using JWH-015 as external standard. When analyzed by LC-MS, both compounds co-elute at 2.80 min (Figure 4a) and are independently detected when monitoring their respective base peaks of 169.0 and 155.0 (Figure 4b and 4c). Resolution of ST-11 and the internal standard, JWH-015, was performed by monitoring parent ions with  $m/z$  328.2 and identifying diagnostic daughter ions with either  $m/z$  169 (cone=43V) or  $m/z$  155 (cone=25V) respectively (Figure 4b-c). ST-11 was quantified in a linear range from 30 fg to 1 ng ( $r^2 > 0.99$ ) after spiking ST-11 into either blood or brain matrix, extracting the compound and injecting the resultant extraction into the HPLC/MS with a fixed amount of internal standard (1 ng JWH-015) (Figure 4d). We calculated the limit of detection (LOD) at 100 fg and limit of quantitation (LOQ) at 3 pg (error <10%). These results indicate that our newly developed method allows for the precise quantification from 0.1 to 1 ng of ST-11 present mouse blood serum and brain tissue.

After determining the quantification limits of ST-11, a time-course pharmacokinetic study was performed that analyzed the concentrations of ST-11 in blood and brain at 10, 30, 60, 90, and 480 min after i.p. administration of 40 mg/kg ST-11 ( $n=2$  per time point). Plasma levels of ST-11 peaked at 10 min ( $15.3 \mu\text{M} \pm 3.6$ ), declined steadily thereafter and reached undetectable levels 8 hrs post-injection (Figure 4e). In contrast, brain ST-11 levels peaked at 60 min post-injection ( $8.7 \pm 0.9 \mu\text{M}$ ) and remained at a concentration exceeding its  $\text{EC}_{50}$  at killing DBT cells for up to 8 hrs ( $1.8 \pm 0.2 \mu\text{M}$ ). We also sought to determine if a lower dose of ST-11 could achieve similarly high concentrations of ST-11 in the brain. Thus, i.p. injections of 5, 15, or 40 mg/kg ST-11 ( $n=2$  per dose) were administered and blood serum and brain were collected 60 min post-injection. These data reveal that the optimal dose of ST-11 was 40 mg/kg, which resulted in brain ST-11 levels above  $\text{EC}_{50}$  for at least 60 min (Figure 4f). These results indicate that formulating ST-11 into liposomes delivers micromolar concentrations of ST-11 to the mouse brain lasting 4-6 hrs.

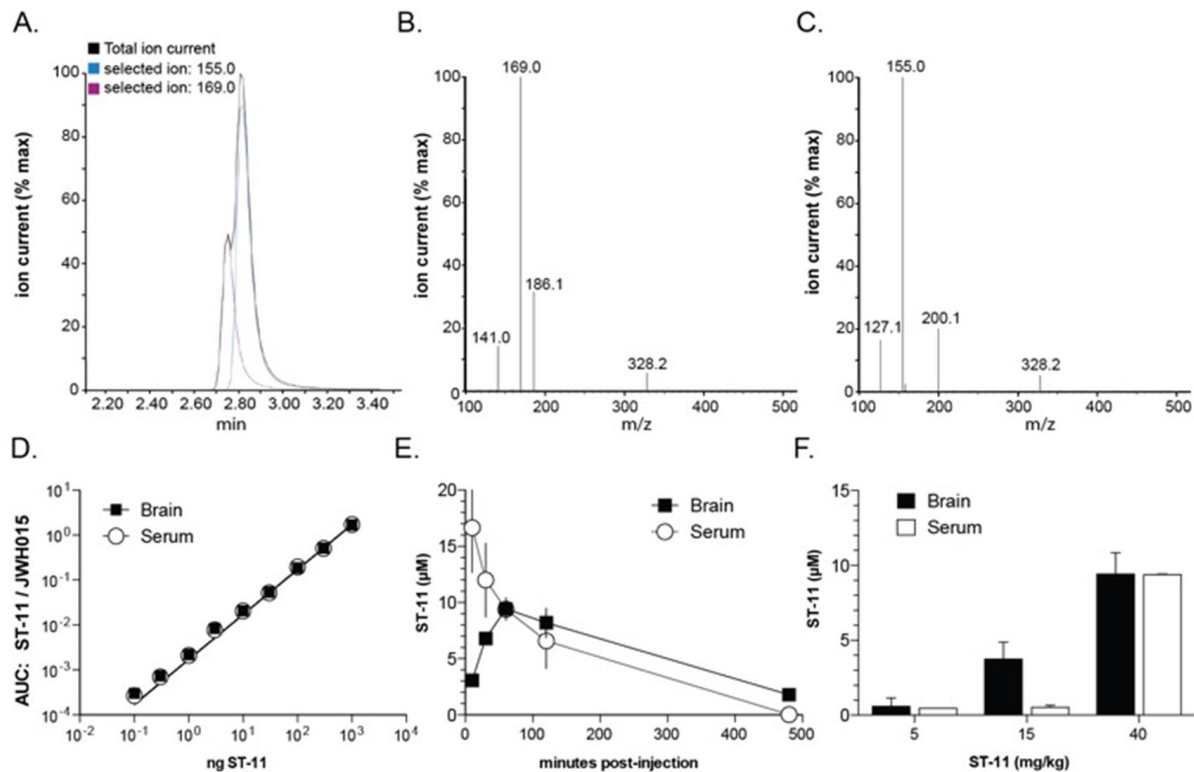


Figure 4: ST-11 formulated in liposomes and injected i.p. reaches the brains of mice. (A-C) ST-11 and JWH-015 co-elute at the same time of 2.80 min. (D) Ratio of ST-11 and JWH-015 detected from brain and serum show that ST-11 can be precisely quantified. (E) PK of ST-11 in serum and brain showing serum peak at 10 min and declining afterwards while brain peak occurs at 60 min and is still detectable at  $1.8 \pm 0.2 \mu\text{M}$  after 8 hrs. (F) Serum and brain samples of mice injected with 5, 15, and 40 mg/kg doses of ST-11 collected after 60 min show that 40 mg/kg is optimal, resulting in therapeutically viable concentrations in the brain.

## ST-11 induces apoptosis in the DBT syngeneic mouse model of astrocytoma

DBT cells develop GBM-like tumors when intracranially-implanted into syngeneic hosts<sup>162,163</sup>. To test the *in vivo* efficacy of ST-11 in this model, mice were implanted with  $10^6$  DBT cells and one week later started daily treatment with vehicle or 5, 15, 40 mg/kg ST-11 for two weeks, at which time all animals were sacrificed to determine if ST-11 had affected tumor growth. Tumor volume was estimated by outlining the tumor mass on H&E sections sampled across the tumor and calculating the approximate volume (see methods). We found that ST-11 treatment induced a dose-dependent reduction of tumor volume (Figure 5a and 5b). To further investigate this response, brain sections containing DBT tumors were immunostained for caspase 3 to determine if apoptosis had been induced by ST-11. Figure 5c-f show progressively increasing levels of activated caspase 3 staining with higher ST-11 doses. High magnification analysis show elevated levels of active caspase 3 in condensed nucleus compared to vehicle-treated controls (inset of Figure 5c-f). These results suggest that the levels reached by ST-11 in mouse brain promote apoptosis in DBT tumors leading to a reduction in tumor volume.

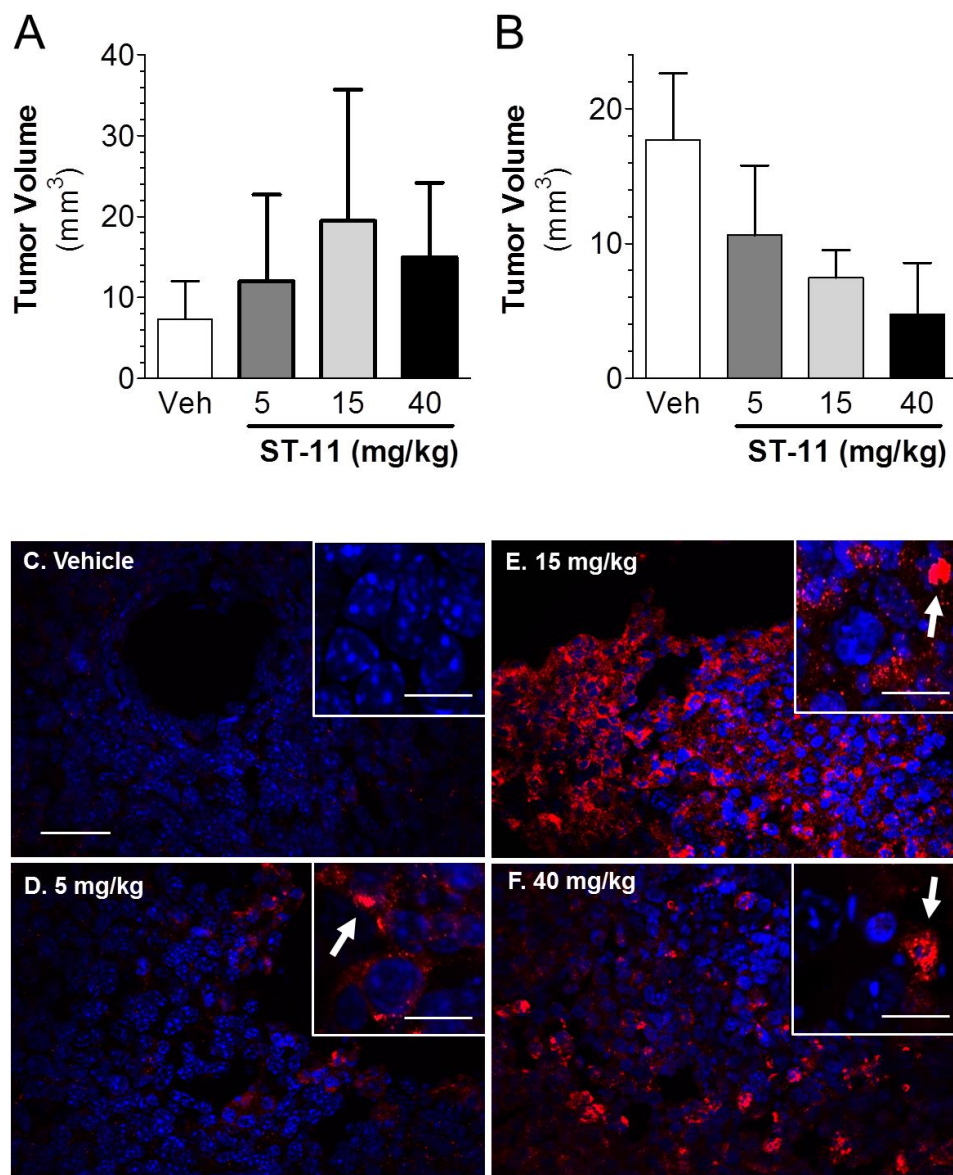


Figure 5: ST-11 reduces DBT tumor volume in vivo involving apoptosis. (A) Quantification in brain slices shows an increase in tumor volume with increasing doses of ST-11. (B) Quantification of tumor volume with volume from Iba1 staining removed shows that ST-11 is negatively affecting DBT tumor cells. (C-F) Representative images of brain slices of mice given (C) vehicle, (D) 5, (E) 15 or, (F) 40 mg/kg ST-11 in liposomes. Arrows pointing to cleaved caspase 3 in tumor cells. Blue = DAPI, red = cleaved caspase 3.

## Tumor-associated macrophages respond to ST-11 treatment

A large number of microglia and macrophages invade and fuel the GBM tumor mass and are referred to as tumor-associated macrophages (TAM) <sup>154,164</sup>. A key feature of a syngeneic mouse model is the presence of an intact immune system that allows for an analysis of TAM. We saw that ST-11 increased tumor volume as a whole, even though caspase 3 activation was present within the tumor. This led us to examine the effects of ST-11 on TAM. When quantifying Iba-1 expression by semi-quantitative-IHC, we found that while Iba-1 expression was only slightly increased in the tumor rim, the density of Iba-1-positive pixels was higher in the tumor rim compared to the contralateral side, a result that correlates with changes in GFAP expression (Figure 6). Together, these results indicate that the rim surrounding DBT tumors is characterized by increases in the density of reactive astrocytes and activated TAM.

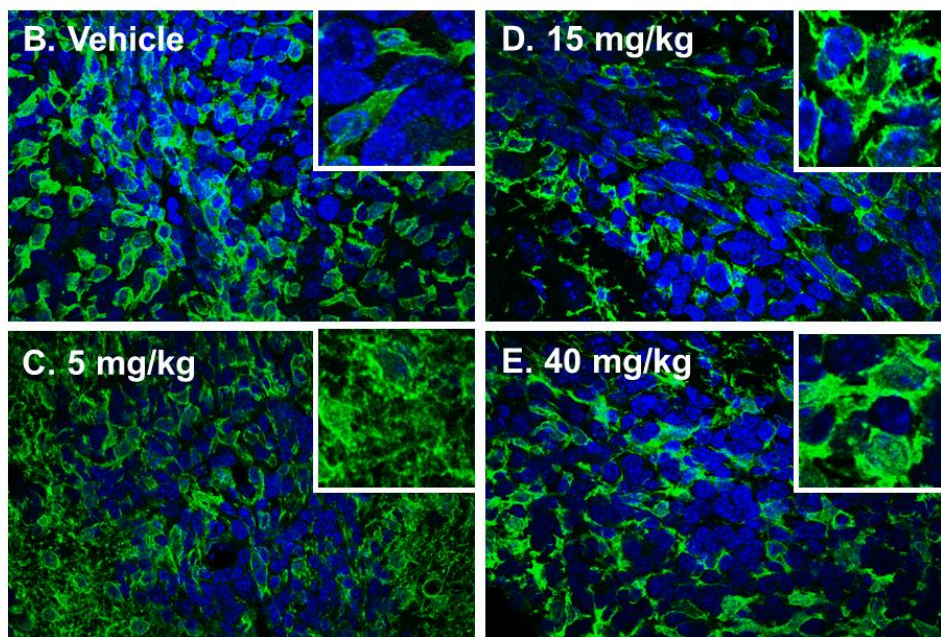
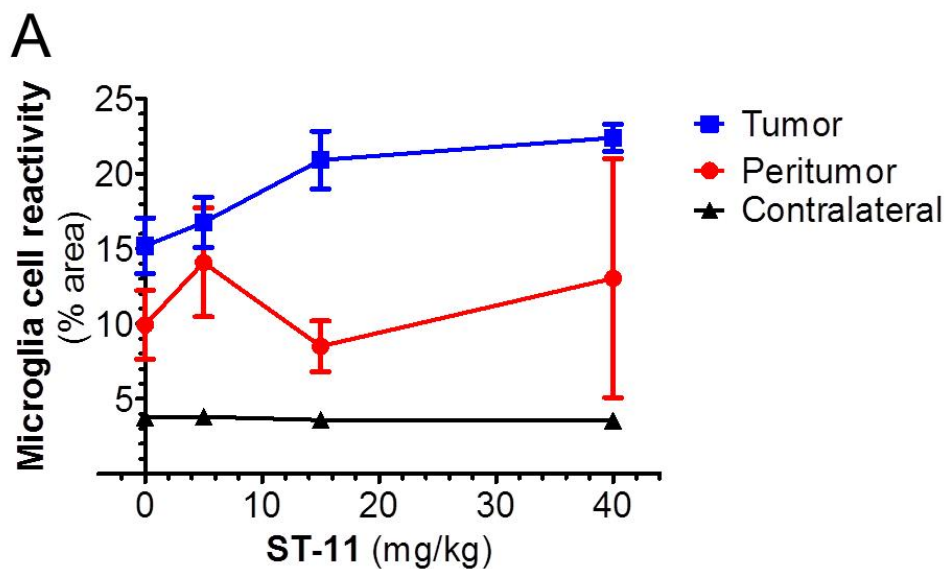


Figure 6: ST-11 in vivo increases activation of TAM. (A) Quantification of Iba-1 staining in different areas of brain showing highest TAM activation within the tumor. (B-E) Representative images of mouse brain slices injected with DBT tumor cells treated with (B) vehicle, (C) 5, (D) 15, or (E) 40 mg/kg ST-11 in liposomes. Images show dose-dependent increase of TAM activation. Blue = DAPI, Green = Iba-1.

## Discussion

Here we show that AI-sensitive receptors are functionally expressed by mouse astrocytoma cells. Ligands activating these receptors in DBT cells in vitro negatively modulate migration stimulated by LPA suggesting that these receptors may play a role in cell invasion and metastasis. In GBM, the increased production of LPA is likely due to the upregulation of autotaxin/lysophospholipase D, which converts lysophosphatidylcholine to LPA. This subsequently was shown to increase cell migration<sup>165</sup>. Our study also shows that AI receptor activation exerts antiproliferative effects by inducing apoptosis. This is in line with many previous studies demonstrating that cannabinoids and alkylindoles induce apoptosis and ultimately reduce tumor size and increase survival time<sup>80,81,85,157,166</sup>. The decrease in proliferation and viability is likely separate from the effect seen with migration as the IC<sub>50</sub> of ST-11 for migration is nearly 2 orders of magnitude lower than it is for proliferation or viability. We note that the EC<sub>50</sub> value measured to induce cell death was significantly different from the binding affinity measured for ST-11 in binding, regulating cell migration and proliferation compared to promoting cell death.

The ability to formulate ST-11 in order to remain stable over a 2 week period represents an important step to implement its in vivo safety and efficacy testing. When ST-11 is administered i.p., it is able to cross the blood brain barrier and reach the brain in concentrations sufficient to activate these novel receptors. In the brain, AI receptor activation increases TAM reactivity while killing tumor cells. The possibility of a compound able to increase microglial cell reactivity is a promising therapeutic outcome as these resident immune cells take on an immunosuppressed phenotype and are not able to kill and remove the tumor cells<sup>28,117</sup>. Other studies have shown that being able to prime microglia to take on a pro-inflammatory phenotype before tumor cells are introduced results in the microglia retaining their ability to kill tumor cells<sup>167</sup>. When coupled with the result that the novel compound also is antiproliferative for tumor cells, while leaving neurons undamaged, treatment with this compound appears to increase immune defense and directly target tumor cells.

The novel ligands developed in our laboratory can be utilized to further characterize this receptor target. Its molecular identity remains unknown at this time as are its endogenous ligands and signaling partners. LPA-stimulated glioma cell migration has been shown to be mediated by phosphorylation of the regulatory light chain of myosin II, resulting in the inhibition of migration<sup>168</sup>. This study shows that these compounds may serve as tools for the development of novel therapies for GBM.

## Materials and Methods

Reagents : ST-11 was synthesized by John W. Huffman at Clemson University, and ST-23, ST-25, ST-29, ST-47, and ST-48 were synthesized at Medchem Source (Seattle, WA). SR141716 and SR144528 was provided by the NIDA drug supply program (RTI International, Research Triangle Park, NC). WIN55212-2 and O-2050 were purchased from Tocris (Minneapolis, MN), isoproterenol was purchased from Sigma (St Louis, MO), and C18:1 LPA was purchased from Avanti Polar Lipids, Inc. (Alabaster, AL). [<sup>3</sup>H]WIN55212-2 and [<sup>3</sup>H]thymidine were purchased from Perkin Elmer (Boston, MA).

Radioligand Binding: DBT membranes were prepared by lysing cells with ice-cold homogenization buffer composed of the following: Tris (50 mM), EDTA (1 mM), and MgCl<sub>2</sub> (3 mM). Lysed cells were homogenized with a Dounce homogenizer (Wheaton Science Products, Millville, NJ). Homogenates were centrifuged at 200 x g for 10 min at 4°C, the supernatant was collected and centrifuged at 45,000 rpm. Supernatant was removed and membrane pellets were stored at -80°C until further use. On the day of experiments, membranes were thawed, and the protein concentration was quantified with the DC protein assay (BioRad, Hercules, CA) using BSA as a standard. All experiments were performed using silanized glass test tubes (Alltech, Deerfield, IL) and silanized pipette tips (VWR Scientific, Brisbane, CA) to minimize the loss of hydrophobic compounds. Binding buffer (pH 7.4) contained the following: Tris-base (50 mM), EDTA (1 mM), MgCl<sub>2</sub> (3 mM), and BSA (1 mg/ml). The following components were added to test tubes placed on ice: 50 µl of binding buffer with compound, 50 µl of binding buffer with radioligand, and 100 µl of binding buffer containing membranes (75 µg of protein). Tubes were then covered and incubated for 1 hr in a 30°C-water bath with mild agitation. Reactions were stopped by rapid filtration using a Brandel harvester (Brandel, Gaithersburg, MD), collecting radioactive membranes on Whatman GFB filter strips (Brandel, Gaithersburg MD), and rinsing with ice-cold binding buffer. Filters were transferred to 7-ml glass scintillation vials (VWR Scientific, Brisbane, CA) using the Brandel Manual Deposit System (Brandel, Gaithersburg, MD), and 4 ml scintillation fluid (National Diagnostics, Atlanta GA; Ecoscint XR) was added to each scintillation vial. Samples were vortexed for 10 sec and followed by 18 hrs incubation at room temperature prior to quantifying radioactivity with a scintillation counter (PerkinElmer, Boston, MA).

Cell Culture & Migration: DBT cells were grown in DMEM supplemented with 10% FBS, 5 mM HEPES, 5 mM NaHCO<sub>3</sub>, 100 U/ml penicillin and 100 µg/mL streptomycin on 100mm dishes (BD Biosciences, San Jose, CA). Cells were used in Boyden chamber migration assays as previously described<sup>120</sup> with minor modifications. Specifically, filters with a pore diameter of 10 µm (Neuroprobe, Gaithersburg, MD) were incubated in

10 ml of a collagen solution (2.5 mg rat tail collagen I (BD Biosciences, San Jose, CA), 57  $\mu$ l glacial acetic acid (Fisher, Santa Clara, CA) in 50 ml distilled water) for 30 min at 37°C. Filters were rinsed 3 times with PBS and allowed to dry before use. Following a 3 hr migration period at 37°C, the scan settings on the Odyssey Infrared Imaging System (LI-COR, Lincoln, NE) were as follows: resolution, 169  $\mu$ m; quality, low; focus offset, 1 mm; and intensity, 4.0.

Cell Viability and Proliferation: DBT cells were plated at a density of  $1.5 \times 10^4$  cells/well in 48-well plates (Corning, Tewksbury, MA) and maintained in normal cell culture conditions for 24 hrs. Cells were treated with ST-compounds and [ $^3$ H]thymidine (PerkinElmer, Waltham, MA) for 72 hrs at 37°C. To measure cell viability concomitantly with cell proliferation, cells were incubated with 10  $\mu$ l WST-1 (Roche, Indianapolis, IN) 60 min before cell lysis and returned to 37°C. The WST-1 absorbance was measured using a SpectraCount BS10000 (PerkinElmer, Waltham, MA.) at a wavelength of 450 nm. Culture media was removed, and cells were rinsed with 250  $\mu$ l ice-cold PBS and lysed with 250  $\mu$ l NaOH (1 M). Cell lysates were kept on ice for 10 min and then transferred to 7-ml glass scintillation vials (VWR Scientific, Brisbane, CA). Distilled H<sub>2</sub>O (250  $\mu$ l) was added to each vial followed by 4 ml scintillation fluid (National Diagnostics, Atlanta GA; Ecoscint XR). Samples were vortexed and radioactivity was measured using a scintillation counter (PerkinElmer, Waltham, MA).

Maximal Tolerated Dose (MTD) and Dose-Range Finding (DRF) Studies: All animal experiments were performed with the approval of the Institutional Animal Care and Use Committee of the University of Washington, Seattle, WA. For the MTD study, CD1 mice (Harlan Laboratories) were injected i.p. with one dose of 5, 15, 40, 80, 160, or 240 mg/kg ST-11 or the corresponding volume of vehicle. Mice were monitored and observed for signs of general distress, organ system dysfunction, and/or moribund state for 24 hours post-injection. Mice that passed the operational definition of tolerable for the MTD study were funneled into the DRF study. In the DRF study, mice were injected once daily i.p. with 5, 15, 40, 80, 160, or 240 mg/kg ST-11 or the corresponding volume of vehicle for 5 days and were monitored as in the MTD study. After completion of MTD and DRF studies, mice were euthanized with ketamine/xylazine mixture (520 and 35.2 mg/kg, respectively), and organs harvested for histopathological analysis.

Extraction and HPLC/MS: Whole brains and 500  $\mu$ L of blood were collected from anesthetized CD1 mice. Blood was collected from the heart and immediately centrifuged at 10,000 rpm to pellet the cellular component, and 200  $\mu$ L plasma was removed. Brains were collected after perfusion with 20 mL of PBS. Freshly dissected tissue samples were homogenized in 10 volumes of CHCl<sub>3</sub>, and these samples were stored at -20°C. 1 mL from each sample was added to a Folch extraction (2 mL CHCl<sub>3</sub>,

1 mL MeOH, 0.5 mL PBS), and 1 µg of JWH-015 was spiked in as an internal control. Samples were vortexed for 1 min and sonicated for 5 min. Following sonication, samples were spun at 500 g for 5 minutes at 4°C to separate the phases. 200 µl of the CHCl<sub>3</sub> phase was removed, dried down under N<sub>2</sub>, and then resuspended in 1 mL of acetonitrile. From this preparation, 10 µl of each sample was injected in a Waters Micromass Quattro Premier XE (Milford, MA) equipped with a C18 column. The HPLC protocol used a fixed flow rate of 0.3 mL\*min<sup>-1</sup>: 1) Initial - 70% ACN, 30% H<sub>2</sub>O. 2) At 2.5 min, ramp to 90% ACN / 10% H<sub>2</sub>O, 3) at 3.5 min, return to 70% ACN / 30% H<sub>2</sub>O, 4) at 4.5 min, end. Using this method, an ST-11 peak was observed at 2.7 min, whereas a JWH-015 peak was observed at 2.9 min. Both ST-11 and JWH-015 have a parent m/z 328.2, therefore ES+ daughter ion analysis was performed to distinguish the compounds with ST-11 at 328->169 and JWH-015 at 328->155. Quantitation was performed by taking a ratio of AUC ST-11/AUCJWH-015, and then calculating the weight of ST-11 using a standard curve.

Immunocytochemistry: Mouse DBT astrocytoma cells were plated on coverslips in DMEM supplemented with 10% FBS and incubated overnight at 37°C in a humidified incubator with 5% CO<sub>2</sub>. The next day, the media was aspirated and replaced with DMEM containing 1% FBS and again incubated overnight. ST-11 or ST-25 was applied to DBT cells and incubated for 6hrs at 37°C. The incubation period was stopped by fixation in 4% PFA for 10 minutes at room temperature (RT). Following fixation, the cells were washed in PBS and permeabilized in 0.02% Triton X-100 for 10 minutes at RT. The cells were blocked in 5% goat serum for 1hr at RT before staining with rabbit anti-human activated caspase-3 antibody (Abcam, Cambridge, MA, 1:250 in 2.5% goat serum) overnight at 4°C. The next day, the cells were washed 3x in PBS for 10 minutes each and incubated with AlexaFluor 555-conjugated goat anti-rabbit secondary antibody (Invitrogen, Grand Island, NY) and DAPI (Invitrogen, Grand Island, NY) (both at 1:500 in 2.5% goat serum) for 1hr at RT. The cells were washed 3 more times in PBS, and coverslips were mounted with fluoromount (Sigma, St Louis, MO). Activated caspase-3 was visualized on an inverted microscope with an Apatome (Zeiss AxioObserver Z1) using a 63x oil-immersion objective.

Statistical Analysis: The GraphPad Prism software version 5.01 was used to conduct statistical analysis. Data are presented as mean ± S.E.M., and statistical significance was measured using one-way ANOVA followed by a post-hoc Dunnett's multiple comparison test or two-tailed t-test.

## Chapter 3: Conclusions

### Summary

To summarize the previous chapters, I have shown evidence for AI-sensitive receptors in microglia and DBT cells. To accomplish this, novel compounds were developed which were used as pharmacological tools. Interestingly, AI receptor activation in both cell types resulted in decreased migration induced by a stimulus. cAMP data from the microglia suggests that the AI receptors are GPCRs. Results from microglia also show that proliferation is dose-dependently inhibited, but only when stimulated by M-CSF. While I could not find any modulation of either M1 or M2 phenotypes in the assays I performed, various parameters can be varied to study phenotype change in more detail. Differences in receptor activation are apparent in proliferation and viability assays. While AI compounds are not harmful to primary microglia or neurons, they do kill DBT cells in micromolar concentrations. ST-11 induced apoptosis in DBT cells, which is a promising outcome that can be explored further in vivo. The presence of AI receptors in both microglia and astrocytoma cells is relevant in GBM as TAMs play an important role in maintaining an environment conducive for tumor survival; perhaps AI receptors can be targeted as part of a therapeutic strategy that provides a better clinical outcome in vivo. The studies performed so far serve as an initial step to understanding how AI receptors may play a role in such a strategy.

### Future directions

Moving forward, there are a number of experiments that can be easily done in a cell line, such as the DBT cells, that would add to the understanding of which moieties are required for AI receptor binding. As new compounds have been synthesized since my introduction to the ST compounds, binding competition curves of the newest and promising compounds would be easily obtainable. Other questions that I am quite enthusiastic about relate to microglial cell response to AI receptor activation.

A basic experiment that remains to be done is to find out how many AI receptors are expressed by microglia, which can be accomplished with saturation binding. This was not done during my graduate career due to availability of resources, described below. It would be worthwhile to continue exploring cell phenotype upon AI receptor activation by looking at NO and cytokine production. Treating microglia primed by IL-4, TGF- $\beta$ , or glioma-conditioned media, with compounds before looking at NO levels is a rational set of experiments to perform, especially if thinking about these cells in a GBM model. The

results may provide a more comprehensive picture as to whether or not M1 phenotype is modulated by ST compound treatment. Looking at cytokine levels is an approach that would yield much more information as one would be able to profile pro-inflammatory as well as anti-inflammatory cytokines, many of which can be done using one set of cells, a benefit of a multiplex assay.

When the next generation of ST compounds becomes available and ready to test in vivo, it will be valuable to allocate a number of animals to look at the cytokine/chemokine profile of whole brains or specifically in FACS-sorted TAMs and compare them between treatment groups. This would provide stronger evidence for the initial IHC data that ST compounds increase TAM reactivity; something missing in the current study. Perhaps the biggest questions that remain to be answered are the identity of the AI receptor, what is its endogenous ligand(s), and whether it is the same receptor in microglia and astrocytoma cells. A sufficiently high-affinity ligand suitable for Click chemistry is the next milestone to achieve as this will allow for the receptor target to remain bound to the ligand and pulled down and perhaps answer this very question.

Working in parallel, elucidating the signaling pathways involved with AI receptor activation is another important aspect of the future direction of this project. Although it is currently being explored in the lab, including looking at ERK and Akt, it is being done in astrocytoma cells. As the results of those experiments are being done and analyzed, it remains to be seen whether the same pathways are activated in TAMs or their non-malignant counterparts, astrocytes and microglia. It will be relevant to discover any correlations between activated signaling pathways and functional readouts that have been collected so far (migration, proliferation, viability). Corroborating data would initially suggest that AI receptor activation leads to the same outcome, for example, the inhibition of stimulated migration in DBT cells and microglia. Opposing data may suggest different mechanisms at work, as evidenced by cell viability data in DBT cells in contrast with microglia and neuron data. This latter result may open questions to signaling differences between malignant and healthy cells.

The molecular mechanism mediating the inhibition of migration needs to be established. In the microglia study, cAMP levels were shown to increase when ST-11 was applied; I did not try to see whether or not this was related to the inhibition of migration stimulated by ATP. Preliminary experiments can be done using various activators of cAMP, such as  $\beta$ -adrenergic receptor agonist isoproterenol or PKA- or Epac-specific activators, as well as antagonists to these receptors/pathways. There is a study published showing that isoproterenol increases cAMP levels via Epac signaling in glioma cell lines, resulting in decreased Rac1 activation and ultimately inhibits migration stimulated by LPA<sup>169</sup>. Although this was done in glioma cell lines, this opens up questions pertaining both to my microglia and DBT findings. The same experiments outlined above can be done in both cell types.

In considering the Boyden chamber migration assay that I have used, I am curious about the results that I may get by varying parameters while preparing the polycarbonate filters or by using other related assays. The Boyden chamber has its advantages because of its ease of use and established protocol within the lab. The substrate by which the filter is coated can be modified from no coating to collagen or Matrigel®. Other filter assays, which utilize filter inserts and cell culture plates might be useful to test as one can easily limit the coating coverage of the filter to the bottom portion, thereby using the coating, or a combination of a compound with the coating, itself as a chemoattractant. The disadvantage here is that more cells will be required to test each condition. Another method to measure migration is the scratch wound assay, which eliminates the need for filters and is easy to set up and has the advantage of being able to take images of the plate at multiple timepoints, thereby gaining information about the speed by which the cells migrate. One clear disadvantage, however, is that any compounds added to the plate will be a bath application as it is not possible to set up a gradient. An assay that would solve that problem is the microfluidics chamber assay, allowing for finer control of the gradient. This is also an advantage over using a Boyden chamber because one would be more confident that the gradient is indeed linear<sup>134</sup>. With any of these assays, one will likely not be able to quantify migrated cells using the lab's current semi-quantitative method and some of them would involve a significant amount of method development.

## Closing remarks

Moving forward with research using cannabinoids and cannabinoid-like compounds is important because there is much that we do not know regarding the therapeutic potential of these compounds to alleviate a wide variety of diseases. Cannabinoids have a bad reputation because of the psychotropic effects attributed to CB<sub>1</sub> activation, but as research has illuminated over the years, the Cannabis plant contains dozens of non-psychotropic compounds that may serve as templates for medicinal chemists to modify, for biologists to test, and ultimately for patients to benefit from. Much of the published research has focused on THC and CBD, a good start, but many opportunities remain to better understand these compounds, alone as well as in combination with other treatments. In an era where personalized medicine is rising to prominence, combinations of treatments need to be tested and optimized. My hope for cannabinoids is that one day we will understand them to a degree where they could be recognized as first-line therapeutics for diseases, such as GBM, rather than therapeutics to treat side-effects of treatment regimens that currently do not confer significant benefit to patients.

While it was exciting to be able to perform the majority of my thesis work using primary microglia in order to use a model “one step above” immortalized cell lines, it was a

challenge to generate enough cells to perform the experiments that I wanted to accomplish. It was not always possible to do full dose-responses for an experiment, or to do an experiment at all. Yet another setback I faced is that for a number of months, the microglia were somehow attaching to the astrocyte layers lining the culture flasks. While this left me without cells to work because they were uncollectable, the silver lining is that I was able to focus my efforts to find out whether ST compounds affected DBT cells. Another drawback of culturing these primary cells on a weekly or bi-weekly basis continuously for nearly the past 6 years is the development of finger and wrist pain. I strongly urge the next person that cultures these cells to take care of their hands in order to keep them in working condition.

Being a part of this graduate program has been an eye-opening experience where I have gained not only knowledge about the fields of neuroscience and pharmacology, but perhaps more importantly, my capabilities as a scientist. I enjoyed learning the various techniques required to work on my project and have put an amount of thought into modifying protocols to get them to work; graduate school was my introduction to working in a wet lab environment. Many mistakes were made, which served as memorable lessons, but out of this, I have emerged with abilities to troubleshoot problems that arise with protocols and equipment. I have thought at times that graduate school provides lessons in crisis management, which sounds dramatic, but it certainly feels like it applies when results to a key experiment are on the line! A big challenge was to overcome the mindset of a (timid) student and transition to becoming an independently-thinking, confident researcher. I had a difficult time with this and am glad this was pointed out to me early on as I was unaware that it was a mental state that I was stuck in. This personal project progresses incrementally, but in a forward direction.

I look forward to the next step of my scientific career, where I can continue researching the interaction between the immune response and its role in various CNS pathologies. Whether it is glioblastoma multiforme or Alzheimer's disease, it is becoming increasingly clear that microglia and other immune cells play a role in disease progression.

## References

1. Thomas, R. P., Recht, L. & Nagpal, S. Advances in the management of glioblastoma : the role of temozolomide and MGMT testing. *Clin. Pharmacol. Adv. Appl.* 5, 1–9 (2013).
2. CBTRUS Fact Sheet. CBTRUS Fact Sheet at <<http://www.cbtrus.org/factsheet/factsheet.html>>
3. Crowley, R. W., Pouratian, N. & Sheehan, J. P. Gamma knife surgery for glioblastoma multiforme. *Neurosurg Focus* 20, 1–5 (2006).
4. Souhami, L. et al. Randomized comparison of stereotactic radiosurgery followed by conventional radiotherapy with carmustine to conventional radiotherapy with carmustine for patients with glioblastoma multiforme: report of Radiation Therapy Oncology Group 93-05 protocol. *Int. J. Radiat. Oncol. Biol. Phys.* 60, 853–60 (2004).
5. Yabroff, K. R., Harlan, L., Zeruto, C., Abrams, J. & Mann, B. Patterns of care and survival for patients with glioblastoma multiforme diagnosed during 2006. *Neuro. Oncol.* 14, 351–9 (2012).
6. Zinn, P. O., Colen, R. R., Kasper, E. M. & Burkhardt, J.-K. Extent of resection and radiotherapy in GBM: A 1973 to 2007 surveillance, epidemiology and end result analysis of 21,783 patients. *Int. J. Oncology* 42, 929–934 (2013).
7. Cohen, M. H., Johnson, J. R. & Pazdur, R. Food and Drug Administration Drug approval summary: temozolomide plus radiation therapy for the treatment of newly diagnosed glioblastoma multiforme. *Clin. Cancer Res.* 11, 6767–71 (2005).
8. Wippold II, F., Lämmle, M., Anatelli, F., Lennerz, J. & Perry, A. Neuropathology for the neuroradiologist: palisades and pseudopalisades. *Am. J. Neuroradiol.* 27, 2037–2041 (2006).
9. Verhaak, R. G. W. et al. Integrated genomic analysis identifies clinically relevant subtypes of glioblastoma characterized by abnormalities in PDGFRA, IDH1, EGFR, and NF1. *Cancer Cell* 17, 98–110 (2010).
10. The Cancer Genome Atlas Network. Comprehensive genomic characterization defines human glioblastoma genes and core pathways. *Nature* 455, 1061–8 (2008).
11. Yuan, X. et al. Isolation of cancer stem cells from adult glioblastoma multiforme. *Oncogene* 23, 9392–400 (2004).

12. Beier, D. et al. CD133(+) and CD133(-) glioblastoma-derived cancer stem cells show differential growth characteristics and molecular profiles. *Cancer Res.* 67, 4010–5 (2007).
13. Liu, G. et al. Analysis of gene expression and chemoresistance of CD133+ cancer stem cells in glioblastoma. *Mol. Cancer* 5, 67 (2006).
14. Singh, S., Hawkins, C., Clarke, I. & Squire, J. Identification of human brain tumour initiating cells. *Nature* 432, 396–401 (2004).
15. Ignatova, T. N. et al. Human cortical glial tumors contain neural stem-like cells expressing astroglial and neuronal markers in vitro. *Glia* 39, 193–206 (2002).
16. Agarwal, S., Sane, R., Oberoi, R., Ohlfest, J. R. & Elmquist, W. F. Delivery of molecularly targeted therapy to malignant glioma, a disease of the whole brain. *Expert Rev. Mol. Med.* 13, e17 (2011).
17. Serwer, L. P. & James, C. D. Challenges in drug delivery to tumors of the central nervous system: an overview of pharmacological and surgical considerations. *Adv. Drug Deliv. Rev.* 64, 590–7 (2012).
18. Noé, B., Hagenbuch, B., Stieger, B. & Meier, P. J. Isolation of a multispecific organic anion and cardiac glycoside transporter from rat brain. *Proc. Natl. Acad. Sci. U. S. A.* 94, 10346–50 (1997).
19. Asaba, H. et al. Blood-brain barrier is involved in the efflux transport of a neuroactive steroid, dehydroepiandrosterone sulfate, via organic anion transporting polypeptide 2. *J. Neurochem.* 75, 1907–16 (2000).
20. Heiss, J. D. et al. Mechanism of dexamethasone suppression of brain tumor-associated vascular permeability in rats. Involvement of the glucocorticoid receptor and vascular permeability factor. *J. Clin. Invest.* 98, 1400–8 (1996).
21. Giometto, B. et al. Immune infiltrates and cytokines in gliomas. *Acta Neurochir. (Wien)*. 138, 50–6 (1996).
22. Schlageter, K. E., Molnar, P., Lapin, G. D. & Groothuis, D. R. Microvessel organization and structure in experimental brain tumors: microvessel populations with distinctive structural and functional properties. *Microvasc. Res.* 58, 312–28 (1999).
23. Seitz, R. J. & Wechsler, W. Immunohistochemical demonstration of serum proteins in human cerebral gliomas. *Acta Neuropathol.* 73, 145–152 (1987).
24. Engelhorn, T. et al. Cellular characterization of the peritumoral edema zone in malignant brain tumors. *Cancer Sci.* 100, 1856–62 (2009).

25. Badie, B. & Schartner, J. M. Flow cytometric characterization of tumor-associated macrophages in experimental gliomas. *Neurosurgery* 46, 957–61; discussion 961–2 (2000).
26. Penfield, W. Microglia and the process of phagocytosis in gliomas. *Am. J. Pathol.* 1, 77–90 (1925).
27. Roggendorf, W., Strupp, S. & Paulus, W. Distribution and characterization of microglia / macrophages in human brain tumors. *Acta Neuropathol* 92, 288–293 (1996).
28. Hussain, S. F. et al. The role of human glioma-infiltrating microglia/macrophages in mediating antitumor immune responses. *Neuro. Oncol.* 8, 261–79 (2006).
29. Kreutzberg, G. W. Microglia: a sensor for pathological events in the CNS. *Trends Neurosci.* 19, 312–8 (1996).
30. Streit, W. J., Walter, S. a & Pennell, N. a. Reactive microgliosis. *Prog. Neurobiol.* 57, 563–81 (1999).
31. Nimmerjahn, A., Kirchhoff, F. & Helmchen, F. Resting microglial cells are highly dynamic surveillants of brain parenchyma in vivo. *Science* 308, 1314–8 (2005).
32. Davalos, D. et al. ATP mediates rapid microglial response to local brain injury in vivo. *Nat. Neurosci.* 8, 752–8 (2005).
33. Ginhoux, F. et al. Fate mapping analysis reveals that adult microglia derive from primitive macrophages. *Science* 330, 841–5 (2010).
34. Prat, E. et al. The human astrocytoma cell line U373MG produces monocyte chemotactic protein (MCP)-1 upon stimulation with beta-amyloid protein. *Neurosci. Lett.* 283, 177–80 (2000).
35. Platten, M. et al. Monocyte chemoattractant protein-1 increases microglial infiltration and aggressiveness of gliomas. *Ann. Neurol.* 54, 388–92 (2003).
36. Okada, M. et al. Tumor-associated macrophage / microglia infiltration in human gliomas is correlated with MCP-3 , but not MCP-1. *Int. J. Oncology* 34, 1621–1627 (2009).
37. Forstreuter, F., Lucius, R. & Mentlein, R. Vascular endothelial growth factor induces chemotaxis and proliferation of microglial cells. *J. Neuroimmunol.* 132, 93–8 (2002).

38. Barleon, B. et al. Migration of human monocytes in response to vascular endothelial growth factor (VEGF) is mediated via the VEGF receptor flt-1. *Blood* 87, 3336–43 (1996).
39. Badie, B., Schartner, J., Klaver, J. & Vorpahl, J. In vitro modulation of microglia motility by glioma cells is mediated by hepatocyte growth factor/scatter factor. *Neurosurgery* 44, 1077–82; discussion 1082–3 (1999).
40. Kunkel, P. et al. Expression and localization of scatter factor/hepatocyte growth factor in human astrocytomas. *Neuro. Oncol.* 3, 82–8 (2001).
41. Tweardy, D. J., Mott, P. L. & Glazer, E. W. Monokine modulation of human astroglial cell production of granulocyte colony-stimulating factor and granulocyte-macrophage colony-stimulating factor. I. Effects of IL-1a and IL-1b. *J. Immunol.* 144, 2233–2241 (1990).
42. Wagner, S. et al. Microglial/macrophage expression of interleukin 10 in human glioblastomas. *Int. J. Cancer* 82, 12–6 (1999).
43. Gabrusiewicz, K. et al. Characteristics of the alternative phenotype of microglia/macrophages and its modulation in experimental gliomas. *PLoS One* 6, e23902 (2011).
44. Markovic, D. S., Glass, R., Synowitz, M., Rooijen, N. Van & Kettenmann, H. Microglia stimulate the invasiveness of glioma cells by increasing the activity of metalloprotease-2. *J. Neuropathol. Exp. Neurol.* 64, 754–62 (2005).
45. Lafuente, J. V et al. Expression of vascular endothelial growth factor (VEGF) and platelet-derived growth factor receptor-beta (PDGFR-beta) in human gliomas. *J. Mol. Neurosci.* 13, 177–85 (1999).
46. Mosser, D. M. & Edwards, J. P. Exploring the full spectrum of macrophage activation. *Nat. Rev. Immunol.* 8, 958–69 (2008).
47. Gordon, S. & Martinez, F. O. Alternative activation of macrophages: mechanism and functions. *Immunity* 32, 593–604 (2010).
48. Saijo, K. & Glass, C. K. Microglial cell origin and phenotypes in health and disease. *Nat. Rev. Immunol.* 11, 775–787 (2011).
49. Hanisch, U.-K. & Kettenmann, H. Microglia: active sensor and versatile effector cells in the normal and pathologic brain. *Nat. Neurosci.* 10, 1387–94 (2007).
50. Parney, I. F., Waldron, J. S. & Parsa, A. T. Flow cytometry and in vitro analysis of human glioma-associated macrophages. Laboratory investigation. *J. Neurosurg.* 110, 572–82 (2009).

51. Charles, N. a, Holland, E. C., Gilbertson, R., Glass, R. & Kettenmann, H. The brain tumor microenvironment. *Glia* 59, 1169–80 (2011).
52. Bodmer, S., Huber, D., Heid, I. & Fontana, a. Human glioblastoma cell derived transforming growth factor-beta 2: evidence for secretion of both high and low molecular weight biologically active forms. *J. Neuroimmunol.* 34, 33–42 (1991).
53. Kjellman, C. et al. Expression of TGF-beta isoforms, TGF-beta receptors, and SMAD molecules at different stages of human glioma. *Int. J. Cancer* 89, 251–8 (2000).
54. Bodmer, S. et al. Immunosuppression and transforming growth factor-beta in glioblastoma. Preferential production of transforming growth factor-beta 2. *J. Immunol.* 143, 3222–9 (1989).
55. Flügel, A., Labeur, M. S., Grasbon-Frodl, E.-M., Kreutzberg, G. W. & Graeber, M. B. Microglia only weakly present glioma antigen to cytotoxic T cells. *Int. J. Dev. Neurosci.* 17, 547–56 (1999).
56. Kettenmann, H., Hanisch, U. K., Noda, M. & Verkhratsky, A. Physiology of microglia. *Physiol. Rev.* 91, 461–553 (2011).
57. McKnight, a J. & Gordon, S. The EGF-TM7 family: unusual structures at the leukocyte surface. *J. Leukoc. Biol.* 63, 271–80 (1998).
58. Matsuda, L. A., Lolait, S. J., Brownstein, M. J., Young, A. C. & Bonner, T. I. Structure of a cannabinoid receptor and functional expression of the cloned cDNA. *Nature* 346, 561–564 (1990).
59. Munro, S., Thomas, K. L. & Abu-Shaar, M. Molecular characterization of a peripheral receptor for cannabinoids. *Nature* 365, 61–65 (1993).
60. Marsicano, G. & Lutz, B. Expression of the cannabinoid receptor CB1 in distinct neuronal subpopulations in the adult mouse forebrain. *Eur. J. Neurosci.* 11, 4213–25 (1999).
61. Steindel, F. et al. Neuron-type specific cannabinoid-mediated G protein signalling in mouse hippocampus. *J. Neurochem.* 124, 795–807 (2013).
62. Glass, M. & Northup, J. K. Agonist selective regulation of G proteins by cannabinoid CB(1) and CB(2) receptors. *Mol. Pharmacol.* 56, 1362–9 (1999).
63. Carlisle, S. J., Marciano-Cabral, F., Staab, a, Ludwick, C. & Cabral, G. a. Differential expression of the CB2 cannabinoid receptor by rodent macrophages and macrophage-like cells in relation to cell activation. *Int. Immunopharmacol.* 2, 69–82 (2002).

64. Van Sickle, M. D. et al. Identification and functional characterization of brainstem cannabinoid CB2 receptors. *Science* (80-. ). 310, 329 (2005).
65. Waksman, Y., Olson, J. M., Carlisle, S. J. & Cabral, G. a. The central cannabinoid receptor (CB1) mediates inhibition of nitric oxide production by rat microglial cells. *J. Pharmacol. Exp. Ther.* 288, 1357–66 (1999).
66. Torres, E. et al. Evidence that MDMA ('ecstasy') increases cannabinoid CB2 receptor expression in microglial cells: role in the neuroinflammatory response in rat brain. *J. Neurochem.* 113, 67–78 (2010).
67. Correa, F. et al. A role for CB2 receptors in anandamide signalling pathways involved in the regulation of IL-12 and IL-23 in microglial cells. *Biochem. Pharmacol.* 77, 86–100 (2009).
68. Gokoh, M. et al. 2-arachidonoylglycerol, an endogenous cannabinoid receptor ligand, induces rapid actin polymerization in HL-60 cells differentiated into macrophage-like cells. *Biochem. J.* 386, 583–9 (2005).
69. Ehrhart, J. et al. Stimulation of cannabinoid receptor 2 (CB2) suppresses microglial activation. *J. Neuroinflammation* 2, 29 (2005).
70. Devane, W. a et al. Isolation and structure of a brain constituent that binds to the cannabinoid receptor. *Science* 258, 1946–9 (1992).
71. Mechoulam, R. et al. Identification of an endogenous 2-monoglyceride, present in canine gut, that binds to cannabinoid receptors. *Biochem. Pharmacol.* 50, 83–90 (1995).
72. Pertwee, R. G. et al. International Union of Basic and Clinical Pharmacology. LXXIX. Cannabinoid Receptors and Their Ligands : Beyond CB1 and CB2. *Pharmacol. Rev.* 62, 588–631 (2010).
73. Stella, N. Cannabinoid and cannabinoid-like receptors in microglia, astrocytes, and astrocytomas. *Glia* 58, 1017–30 (2010).
74. Rinaldi-Carmona, M. et al. SR141716A, a potent and selective antagonist of the brain cannabinoid receptor. *FEBS Lett.* 350, 240–244 (1994).
75. Rinaldi-Carmona, M. et al. SR 144528, the first potent and selective antagonist of the CB2 cannabinoid receptor. *J. Pharmacol. Exp. Ther.* 284, 644–650 (1998).
76. Pertwee, R. G. Cannabinoid pharmacology: the first 66 years. *Br. J. Pharmacol.* 147 Suppl , S163–71 (2006).

77. Cabral, G. & Griffin-Thomas, L. Cannabinoids as therapeutic agents for ablating neuroinflammatory disease. *Endocr. Metab. Immune Disord. Drug Targets* 8, 159 (2008).
78. Velasco, G., Sánchez, C. & Guzmán, M. Towards the use of cannabinoids as antitumour agents. *Nat. Rev. Cancer* 12, 436–444 (2012).
79. Munson, A. E., Harris, L. S., Friedman, M. A., Dewey, W. L. & Carchman, R. A. Antineoplastic activity of cannabinoids. *J. Natl. Cancer Inst.* 55, 597–602 (1975).
80. Galve-Roperh, I. et al. Anti-tumoral action of cannabinoids: involvement of sustained ceramide accumulation and extracellular signal-regulated kinase activation. *Nat. Med.* 6, 313–9 (2000).
81. Guzmán, M. et al. A pilot clinical study of Delta9-tetrahydrocannabinol in patients with recurrent glioblastoma multiforme. *Br. J. Cancer* 95, 197–203 (2006).
82. Marcu, J. P. et al. Cannabidiol enhances the inhibitory effects of delta9-tetrahydrocannabinol on human glioblastoma cell proliferation and survival. *Mol. Cancer Ther.* 9, 180–9 (2010).
83. Cudaback, E., Marrs, W., Moeller, T. & Stella, N. The expression level of CB1 and CB2 receptors determines their efficacy at inducing apoptosis in astrocytomas. *PLoS One* 5, e8702 (2010).
84. Salazar, M. et al. Cannabinoid action induces autophagy-mediated cell death through stimulation of ER stress in human glioma cells. *J. Clin. Invest.* 119, 1359–1372 (2009).
85. Aguado, T. et al. Cannabinoids induce glioma stem-like cell differentiation and inhibit gliomagenesis. *J. Biol. Chem.* 282, 6854–62 (2007).
86. Lorente, M. et al. Stimulation of ALK by the growth factor midkine renders glioma cells resistant to autophagy-mediated cell death. *Autophagy* 7, 1071–1073 (2011).
87. Torres, S. et al. A combined preclinical therapy of cannabinoids and temozolomide against glioma. *Mol. Cancer Ther.* 10, 90–103 (2011).
88. Ramirez, S. H. et al. Activation of cannabinoid receptor 2 attenuates leukocyte-endothelial cell interactions and blood-brain barrier dysfunction under inflammatory conditions. *J. Neurosci.* 32, 4004–16 (2012).
89. Schley, M. et al. Predominant CB2 receptor expression in endothelial cells of glioblastoma in humans. *Brain Res. Bull.* 79, 333–7 (2009).

90. Romero-Sandoval, E. A., Horvath, R., Landry, R. P. & DeLeo, J. a. Cannabinoid receptor type 2 activation induces a microglial anti-inflammatory phenotype and reduces migration via MKP induction and ERK dephosphorylation. *Mol. Pain* 5, 25 (2009).
91. Franklin, A., Parmentier-Batteur, S., Walter, L., Greenberg, D. a & Stella, N. Palmitoylethanolamide increases after focal cerebral ischemia and potentiates microglial cell motility. *J. Neurosci.* 23, 7767–75 (2003).
92. Montecucco, F., Burger, F., Mach, F. & Steffens, S. CB2 cannabinoid receptor agonist JWH-015 modulates human monocyte migration through defined intracellular signaling pathways. *Am. J. Physiol. Heart Circ. Physiol.* 294, H1145–55 (2008).
93. Walter, L., Franklin, A., Witting, A. & Wade, C. Nonpsychotropic cannabinoid receptors regulate microglial cell migration. *J. Neurosci.* 23, 1398–1405 (2003).
94. Monory, K. et al. Novel, not adenylyl cyclase-coupled cannabinoid binding site in cerebellum of mice. *Biochem. Biophys. Res. Commun.* 292, 231–5 (2002).
95. Breivogel, C. S., Griffin, G., Di Marzo, V. & Martin, B. R. Evidence for a new G protein-coupled cannabinoid receptor in mouse brain. *Mol. Pharmacol.* 60, 155–63 (2001).
96. Marzo, V. Di et al. Levels , Metabolism , and Pharmacological Activity of Anandamide in CB 1 Cannabinoid Receptor Knockout Mice : Evidence for Non-CB1, Non-CB2 Receptor-Mediated Actions of Anandamide in Mouse Brain. *J. Neurochem.* 75, 2434–2444 (2000).
97. Hajos, N., Ledent, C. & Freund, T. Novel cannabinoid-sensitive receptor mediates inhibition of glutamatergic synaptic transmission in the hippocampus. *Neuroscience* 106, 6–9 (2001).
98. Franklin, A. & Stella, N. Arachidonylcyclopropylamide increases microglial cell migration through cannabinoid CB2 and abnormal-cannabidiol-sensitive receptors. *Eur. J. Pharmacol.* 474, 195–198 (2003).
99. Sánchez, C., Galve-Roperh, I., Canova, C., Brachet, P. & Guzmán, M. Delta9-tetrahydrocannabinol induces apoptosis in C6 glioma cells. *FEBS Lett.* 436, 6–10 (1998).
100. Jacobsson, S. O., Wallin, T. & Fowler, C. J. Inhibition of rat C6 glioma cell proliferation by endogenous and synthetic cannabinoids. Relative involvement of cannabinoid and vanilloid receptors. *J. Pharmacol. Exp. Ther.* 299, 951–9 (2001).

101. Baker, D., Pryce, G., Davies, W. L. & Hiley, C. R. In silico patent searching reveals a new cannabinoid receptor. *Trends Pharmacol. Sci.* 27, 1–4 (2006).
102. Oka, S., Nakajima, K., Yamashita, A., Kishimoto, S. & Sugiura, T. Identification of GPR55 as a lysophosphatidylinositol receptor. *Biochem. Biophys. Res. Commun.* 362, 928–34 (2007).
103. Whyte, L. S. et al. The putative cannabinoid receptor GPR55 affects osteoclast function in vitro and bone mass in vivo. *Proc. Natl. Acad. Sci. U. S. A.* 106, 16511–6 (2009).
104. Ryberg, E. et al. The orphan receptor GPR55 is a novel cannabinoid receptor. *Br. J. Pharmacol.* 152, 1092–101 (2007).
105. Andradas, C. et al. The orphan G protein-coupled receptor GPR55 promotes cancer cell proliferation via ERK. *Oncogene* 30, 245–52 (2011).
106. Balenga, N. a B. et al. GPR55 regulates cannabinoid 2 receptor-mediated responses in human neutrophils. *Cell Res.* 21, 1452–69 (2011).
107. Lauckner, J. E. et al. GPR55 is a cannabinoid receptor that increases intracellular calcium and inhibits M current. *Proc. Natl. Acad. Sci. U. S. A.* 105, 2699–704 (2008).
108. Pietr, M. et al. Differential changes in GPR55 during microglial cell activation. *FEBS Lett.* 583, 2071–6 (2009).
109. Gantz, I. et al. Cloning and chromosomal localization of a gene (GPR18) encoding a novel seven transmembrane receptor highly expressed in spleen and testis. *Genomics* 42, 462–6 (1997).
110. McHugh, D., Tanner, C., Mechoulam, R., Pertwee, R. G. & Ross, R. A. Inhibition of human neutrophil chemotaxis by endogenous cannabinoids and phytocannabinoids: evidence for a site distinct from CB1 and CB2. *Mol. Pharmacol.* 73, 441 (2008).
111. McHugh, D. et al. N-arachidonoyl glycine, an abundant endogenous lipid, potently drives directed cellular migration through GPR18, the putative abnormal cannabidiol receptor. *BMC Neurosci.* 11, 44 (2010).
112. Kohno, M. et al. Identification of N-arachidonoylglycine as the endogenous ligand for orphan G-protein-coupled receptor GPR18. *Biochem. Biophys. Res. Commun.* 347, 827–32 (2006).

113. Bradshaw, H. B. et al. The endocannabinoid anandamide is a precursor for the signaling lipid N-arachidonoyl glycine by two distinct pathways. *BMC Biochem.* 10, 14 (2009).
114. Succar, R., Mitchell, V. a & Vaughan, C. W. Actions of N-arachidonoyl-glycine in a rat inflammatory pain model. *Mol. Pain* 3, 24 (2007).
115. Huang, S. M. et al. Identification of a new class of molecules, the arachidonyl amino acids, and characterization of one member that inhibits pain. *J. Biol. Chem.* 276, 42639–44 (2001).
116. Ribot, E. et al. Microglia used as vehicles for both inducible thymidine kinase gene therapy and MRI contrast agents for glioma therapy. *Cancer Gene Ther.* 14, 724–737 (2007).
117. Zhai, H., Heppner, F. L. & Tsirka, S. E. Microglia/macrophages promote glioma progression. *Glia* 59, 472–85 (2011).
118. Ribot, E. J. et al. In vivo MR tracking of therapeutic microglia to a human glioma model. *NMR Biomed.* 24, 1361–8 (2011).
119. Ousman, S. S. & Kubes, P. Immune surveillance in the central nervous system. *Nat. Neurosci.* 15, 1096–1101 (2012).
120. Miller, A. M. & Stella, N. Microglial cell migration stimulated by ATP and C5a involve distinct molecular mechanisms: quantification of migration by a novel near-infrared method. *Glia* 57, 875–83 (2009).
121. Lambert, C., Ase, A. R., Séguéla, P. & Antel, J. P. Distinct migratory and cytokine responses of human microglia and macrophages to ATP. *Brain. Behav. Immun.* 24, 1241–8 (2010).
122. Haynes, S. E. et al. The P2Y<sub>12</sub> receptor regulates microglial activation by extracellular nucleotides. *Nat. Neurosci.* 9, 1512–9 (2006).
123. Carrier, E. J. et al. Cultured rat microglial cells synthesize the endocannabinoid 2-arachidonoylglycerol, which increases proliferation via a CB<sub>2</sub> receptor-dependent mechanism. *Mol. Pharmacol.* 65, 999–1007 (2004).
124. Luongo, L. et al. 1-(2',4'-dichlorophenyl)-6-methyl-N-cyclohexylamine-1,4-dihydroindeno[1,2-c]pyrazole-3-carboxamide, a novel CB<sub>2</sub> agonist, alleviates neuropathic pain through functional microglial changes in mice. *Neurobiol. Dis.* 37, 177–85 (2010).

125. Kallendrusch, S. et al. The G protein-coupled receptor 55 ligand  $\text{l-}\alpha\text{-lysophosphatidylinositol}$  exerts microglia-dependent neuroprotection after excitotoxic lesion. *Glia* 61, 1822–31 (2013).
126. Chao, C. C. et al. Activation of mu opioid receptors inhibits microglial cell chemotaxis. *J. Pharmacol. Exp. Ther.* 281, 998–1004 (1997).
127. *EndoCANNABINOIDS: Actions at non CB1/CB2 cannabinoid receptors.* (Springer, 2012).
128. Kozela, E. et al. Cannabinoids Delta(9)-tetrahydrocannabinol and cannabidiol differentially inhibit the lipopolysaccharide-activated NF-kappaB and interferon-beta/STAT proinflammatory pathways in BV-2 microglial cells. *J. Biol. Chem.* 285, 1616–26 (2010).
129. Kozela, E. et al. Cannabinoids decrease the Th17 inflammatory autoimmune phenotype. *J. Neuroimmune Pharmacol.* 8, 1265–76 (2013).
130. Huffman, J. W. & Padgett, L. W. Recent Developments in the Medicinal Chemistry of Cannabimimetic Indoles, Pyrroles and Indenes. *Curr. Med. Chem.* 12, 1395–1411 (2005).
131. Sexton, M. et al. NIR-*mbc94*, a fluorescent ligand that binds to endogenous CB(2) receptors and is amenable to high-throughput screening. *Chem. Biol.* 18, 563–8 (2011).
132. Falkenburger, B. H., Dickson, E. J. & Hille, B. Quantitative properties and receptor reserve of the DAG and PKC branch of G(q)-coupled receptor signaling. *J. Gen. Physiol.* 141, 537–55 (2013).
133. Miller, A. M. & Stella, N. CB2 receptor-mediated migration of immune cells: it can go either way. *Br. J. Pharmacol.* 153, 299–308 (2008).
134. Wilkinson, P. C. Assays of leukocyte locomotion and chemotaxis. *J. Immunol. Methods* 216, 139–53 (1998).
135. Berridge, M. V, Herst, P. M. & Tan, A. S. Tetrazolium dyes as tools in cell biology: new insights into their cellular reduction. *Biotechnol. Annu. Rev.* 11, 127–52 (2005).
136. Derocq, J. M., Ségui, M., Marchand, J., Le Fur, G. & Casellas, P. Cannabinoids enhance human B-cell growth at low nanomolar concentrations. *FEBS Lett.* 369, 177–182 (1995).

137. Théry, C. & Mallat, M. Influence of interleukin-1 and tumor necrosis factor alpha on the growth of microglial cells in primary cultures of mouse cerebral cortex: involvement of colony-stimulating factor 1. *Neurosci. Lett.* 150, 195–9 (1993).
138. Imai, Y. & Kohsaka, S. Intracellular signaling in M-CSF-induced microglia activation: role of Iba1. *Glia* 40, 164–74 (2002).
139. Colton, C. a. Heterogeneity of microglial activation in the innate immune response in the brain. *J. neuroimmune Pharmacol.* 4, 399–418 (2009).
140. Vanguri, P. & Farber, J. M. IFN and Virus-Inducible Expression of an Immediate Early Gene, *crg-2/IP-10*, and a Delayed Gene, *I-Aa*, in Astrocytes and Microglia. *J. Immunol.* 152, 1411–1418 (1994).
141. Hua, L. L. & Lee, S. C. Distinct patterns of stimulus-inducible chemokine mRNA accumulation in human fetal astrocytes and microglia. *Glia* 30, 74–81 (2000).
142. Raes, G. et al. FIZZ1 and Ym as Tools to Discriminate between Differentially Activated Macrophages. *Dev. Immunol.* 9, 151–159 (2002).
143. Facchinetti, F., Del Giudice, E., Furegato, S., Passarotto, M. & Leon, A. Cannabinoids ablate release of TNFalpha in rat microglial cells stimulated with lipopolysaccharide. *Glia* 41, 161–8 (2003).
144. Kreutz, S. et al. 2-Arachidonoylglycerol elicits neuroprotective effects on excitotoxically lesioned dentate gyrus granule cells via abnormal-cannabidiol-sensitive receptors on microglial cells. *Glia* 57, 286–94 (2009).
145. Puffenbarger, R. a., Boothe, A. C. & Cabral, G. a. Cannabinoids Inhibit LPS-Inducible Cytokine mRNA Expression in Rat Microglia Cells. *Glia* 29, 58–69 (2000).
146. Inoue, K. Microglial activation by purines and pyrimidines. *Glia* 40, 156–63 (2002).
147. Thelen, M. Dancing to the tune of chemokines. *Nat. Immunol.* 2, 129–34 (2001).
148. Dustin, M. L., Bromley, S. K., Kan, Z., Peterson, D. a & Unanue, E. R. Antigen receptor engagement delivers a stop signal to migrating T lymphocytes. *Proc. Natl. Acad. Sci. U. S. A.* 94, 3909–13 (1997).
149. Fraga, D., Raborn, E. S., Ferreira, G. a & Cabral, G. a. Cannabinoids inhibit migration of microglial-like cells to the HIV protein Tat. *J. neuroimmune Pharmacol.* 6, 566–77 (2011).
150. Ferreira, R. et al. Neuropeptide Y inhibits interleukin-1 beta (IL-1 $\beta$ )-induced microglia motility. *J. Neurochem.* 120, 93–105 (2012).

151. Bouaboula, M. et al. Signaling pathway associated with stimulation of CB2 peripheral cannabinoid receptor. Involvement of both mitogen-activated protein kinase and induction of Krox-24 expression. *Eur. J. Biochem.* 237, 704–11 (1996).
152. Carrier, E. J., Auchampach, J. a & Hillard, C. J. Inhibition of an equilibrative nucleoside transporter by cannabidiol: a mechanism of cannabinoid immunosuppression. *Proc. Natl. Acad. Sci. U. S. A.* 103, 7895–900 (2006).
153. Turner, R. C., Dodson, S. C., Rosen, C. L. & Huber, J. D. The science of cerebral ischemia and the quest for neuroprotection: navigating past failure to future success. *J. Neurosurg.* 118, 1072–85 (2013).
154. Fung, S. & Stella, N. Targeting endocannabinoid signaling in tumor-associated macrophages as treatment for glioblastoma multiforme. *WIREs Membr. Transp. Signal.* 3, 39–51 (2014).
155. Walter, L., Franklin, A., Witting, A., Moller, T. & Stella, N. Astrocytes in culture produce anandamide and other acylethanolamides. *J. Biol. Chem.* 277, 20869–76 (2002).
156. Ostrom, Q. T. et al. CBTRUS statistical report: Primary brain and central nervous system tumors diagnosed in the United States in 2006-2010. *Neuro. Oncol.* 15 Suppl 2, ii1–56 (2013).
157. Sánchez, C. et al. Inhibition of glioma growth in vivo by selective activation of the CB2 cannabinoid receptor. *Cancer Res.* 5784–5789 (2001). at <http://cancerres.aacrjournals.org/content/61/15/5784.short>
158. Rodriguez, M. a et al. Vincristine sulfate liposomes injection (Marqibo) in heavily pretreated patients with refractory aggressive non-Hodgkin lymphoma: report of the pivotal phase 2 study. *Cancer* 115, 3475–82 (2009).
159. Barenholz, Y. Doxil®--the first FDA-approved nano-drug: lessons learned. *J. Control. Release* 160, 117–34 (2012).
160. Hermanns-Clausen, M., Kneisel, S., Szabo, B. & Auwärter, V. Acute toxicity due to the confirmed consumption of synthetic cannabinoids: clinical and laboratory findings. *Addiction* 108, 534–44 (2013).
161. Young, A. C. et al. Cardiotoxicity associated with the synthetic cannabinoid, K9, with laboratory confirmation. *Am. J. Emerg. Med.* 30, 1320.e5–7 (2012).
162. Sherburn, E. W. et al. Gliomas in rodent whisker barrel cortex: a new tumor model. *J. Neurosurg.* 91, 814–21 (1999).

163. Won, E. K., Zahner, M. C., Grant, E. A., Gore, P. & Chicoine, M. R. Analysis of the antitumoral mechanisms of lipopolysaccharide against glioblastoma multiforme. *Anticancer. Drugs* 14, 457–466 (2003).
164. Bach, J.-P. et al. The role of macrophage inhibitory factor in tumorigenesis and central nervous system tumors. *Cancer* 115, 2031–40 (2009).
165. Kishi, Y. et al. Autotaxin is overexpressed in glioblastoma multiforme and contributes to cell motility of glioblastoma by converting lysophosphatidylcholine to lysophosphatidic acid. *J. Biol. Chem.* 281, 17492–500 (2006).
166. Massi, P., Vaccani, A. & Ceruti, S. Antitumor effects of cannabidiol, a nonpsychoactive cannabinoid, on human glioma cell lines. *J. Pharmacol. Exp. Ther.* 308, 838–845 (2004).
167. Kees, T. et al. Microglia isolated from patients with glioma gain antitumor activities on poly (I:C) stimulation. *Neuro. Oncol.* 14, 64–78 (2011).
168. Manning, T. J., Parker, J. C. & Sontheimer, H. Role of lysophosphatidic acid and rho in glioma cell motility. *Cell Motil. Cytoskeleton* 45, 185–99 (2000).
169. Malchinkhuu, E. et al. Role of Rap1B and Tumor Suppressor PTEN in the Negative Regulation of Lysophosphatidic Acid — induced Migration by Isoproterenol in Glioma Cells. *Mol. Biol. Cell* 20, 5156–5165 (2009).